REMOTE SENS ENVIRON 42 187–216 (1992)

Canopy Reflectance, Photosynthesis, and Transpiration. III. A Reanalysis Using Improved Leaf Models and a New Canopy Integration Scheme.

P. J. Sellers, J. A. Berry,† G. J. Collatz,† C. B. Field,† and F. G. Hall**

**NASA/Goddard Space Flight Center, Greenbelt and †Carnegie Institution, Stanford, California*

The theoretical analyses of Sellers (1985, 1987), which linked canopy spectral reflectance properties to (unstressed) photosynthetic rates and conductances, are critically reviewed and significant shortcomings are identified These are addressed in this article principally through the incorporation of a more sophisticated and realistic treatment of leaf physiological processes within a new canopy integration scheme It is assumed, based on ecophysiological observations and arguments, that leaf physiological properties vary throughout the plant canopy in response to the radiation-weighted time-mean profile of photosynthetically active radiation (PAR) These modifications yield a simpler and more robust theoretical relationship between canopy biophysical rates (photosynthesis, conductance) and spectral vegetation indices (SVI) The results indicate that area-averaged SVI, as obtained from coarse resolution satellite sensors, may give good estimates of the area-integrals of photosynthesis and conductance even for spatially heterogenous (though physiologically uniform) vegetation covers

Address correspondence to Piers Sellers, NASA / GSPC, Code 923, Greenbelt, MD 20771

Received 6 May 1991, revised 28 March 1992

INTRODUCTION

Over the last 10 years, there have been some important advances in our understanding of how leaves assimilate carbon and control the simultaneous loss of water vapor through their stomata Farquhar et al (1980) showed how a biochemical model of leaf CO_2 assimilation based on rate constants calculated from a consideration of the enzyme kinetics and electron transport properties of chloroplasts could yield a realistic description of photosynthesis for C_3 plants Collatz et al (1991), following Ball (1988), used this work and observations of stomatal conductance to construct a robust semiempirical model of leaf stomatal function which can reproduce the response of leaf conductance to changes in ambient temperature, humidity, CO_2 concentration, and assimilation rate A number of investigators (Field, 1983, Terashima and Inoue, 1985, Hirose and Werger, 1987, Gutschick and Wiegel, 1988, Farquhar, 1989, Evans, 1989a) explored consequences of the distribution of photosynthetic capacity in leaves and canopies with respect to light and developed criteria for identifying the distribution of any fixed total capacity that maximizes photosynthetic CO_2 assimilation

It would be useful to extend this knowledge

0034-4257/92/$5 00

655 Avenue of the Americas, New York, NY 10010

of leaf-level processes up to the canopy scale (meters and kilometers) Among other applications, this could lead to the calculation of carbon fluxes and evapotranspiration rates on scales consistent with global biogeochemical cycle studies, see, for example, Tans et al (1990) To do this, it is necessary to quantify the relationships between canopy function and spectral signatures because satellite remote sensing offers the only practical means of continuously and consistently monitoring biospheric processes on a global scale

Sellers (1985, 1987) investigated methods of integrating simple leaf-level models of light scattering, light absorption, photosynthesis, and stomatal conductance over the depth of vegetation canopies His analysis explored a theoretical basis for analyzing the empirical connections between spectral vegetation indices (SVI) and important functional relationships that regulate canopy photosynthesis and transpiration A key result showed that for horizontally uniform (plane-parallel) canopies, there is a strong mechanistic basis for a correlation between the fraction of photosynthetically active radiation absorbed by the vegetation canopy (FPAR) and the associated simple ratio vegetation index (SR) (near-infrared reflectance divided by visible reflectance) The analysis also showed that the bulk canopy photosynthetic capacity and the maximum canopy conductance were near-linearly related to the SR However, the leaf physiological models used in the analysis of Sellers (1985, 1987) suffered from a number of shortcomings

i The leaf CO_2 assimilation and stomatal conductance models used simple empirical functions which are hard to parameterize
ii There was no linkage between stomatal function and leaf CO_2 assimilation
iii Leaf physiological properties (photosynthetic capacity, etc) were assumed to be invariant through the depth of the canopy

These issues are addressed in the analysis presented in this paper We demonstrate that the incorporation of a more sophisticated treatment of physiological processes results in a simpler and more robust relationship between canopy biophysical rates (photosynthesis, conductance) and spectral vegetation indices (SVI)

THEORETICAL BACKGROUND

Summary of the Analysis of Sellers (1985; 1987)

Many researchers have utilized combinations of spectral radiance observations acquired over vegetated surfaces by satellite or aircraft-mounted sensors as indicators of the density, health, or biomass of the vegetation These empirical applications of remote sensing take advantage of the large difference between the light scattering properties of green leaves in the visible and near-infrared wavelength intervals

Sellers (1985, 1987) used a two-stream approximation model to describe radiative transfer within vegetation canopies The equations obtained from the two-stream method may be used to calculate the hemispheric reflectance of a plant canopy as a function of a) the relative spectral response function of the sensor, b) the radiation field incident on the canopy, c) the soil or background reflectance, d) the scattering coefficients and geometric arrangement of the leaf elements, and e) the amount of vegetation present, as specified by the leaf area index, for example A related procedure was used to calculate the profiles of radiation absorbed by leaves as a function of canopy depth

Sellers (1987) used these equations to show that for ideal conditions—uniform green canopy, dark underlying surface—the spectral vegetation indices (SVI) should be proportional to the near-infrared reflectance, a_N, and to FPAR [referred to as APAR in Sellers (1985, 1987)] The most commonly used SVI are the simple ratio (SR) and the normalized difference (ND) vegetation indices, defined as

$$\mathrm{SR} = \frac{a_N}{a_v}, \tag{1a}$$

$$\mathrm{ND} = \frac{a_N - a_v}{a_N + a_v} \tag{1b}$$

where

a_N, a_v = hemispheric canopy reflectances for near-infrared and visible wavelength intervals, respectively (sensor-dependent)

Sellers (1987) showed that this useful relationship between the SVI and FPAR holds because the broad-band scattering coefficients of green leaves in the near-infrared (ω_N) and visible (ω_v)

wavelength intervals are very different (Table 1), this difference is such that

$$\frac{\partial a_N}{\partial L_T} \propto \frac{\partial (\text{FPAR})}{\partial L_T}, \quad \text{for all values of } L_T, \tag{2}$$

where

L_T = total leaf area index

when the extinction coefficient for the flux of PAR or visible radiation (k) is roughly double the extinction coefficient for diffuse near-infrared flux (h_N) within the canopy, that is, when

$$k \simeq 2h_N, \tag{3a}$$

which may be reexpressed as

$$\frac{G(\mu)}{\mu}(1-\omega_V)^{1/2} = 2(-\omega_N)^{1/2}, \tag{3b}$$

where

ω_V, ω_N = leaf scattering coefficients in the visible, near-infrared wavelength intervals, respectively (sensor-dependent),

k = extinction coefficient for direct (solar) beam flux within the canopy $= [G(\mu)/\mu](1-\omega_V)^{1/2}$,

h_N = extinction coefficient for diffuse near-infrared flux within the canopy $= (1-\omega_N)^{1/2}$,

Table 1 Parameters Used To Calculate Leaf Photosynthesis and Conductance for the Models Used in Sellers (1985, 1987)

Parameter	*Units*	*Value*
Photosynthesis		
a_1	μmol m^{-2} s^{-1}	52 0
b_1	μmol m^{-2} s^{-1}, W m^{-2}	1380 0, 300 0
Conductance		
a_2	μmol mol^{-1}, J m^{-3}	1268 5, 13966 0
b_2	μmol m^{-2} s^{-1}, W m^{-2}	0 46, 0 1
c_2	(mol m^{-2} s^{-1})$^{-1}$, s m^{-1}	0 55, 28 0
Leaf properties		
$G(\mu)$	–	0 5
ω_L	–	0 2
ω_N	–	0 95
Soil reflectance		
ω_s	–	0 1
Solar angle		
μ	cos^{-1}	0 5

[a] Adapted from Charles-Edwards and Ludwig (1974) and Jarvis (1976), see Eq (1)

These parameters were obtained by curve fits to the PAR response functions as given by the Farquhar et al (1980) and Collatz et al (1991) models for stress-free (relative humidity = 1) conditions, see Figure 6e, f

$G(\mu)$ = relative projected area of leaves in direction cos$^{-1}\mu$,

μ = cosine of solar zenith angle

Simply put, Eq (2) holds because the near-infrared reflectance a_N is proportional to *double* the pathlength of near-infrared radiation in the canopy [$e^{-2h_N L_T}$], as this radiation must enter *and* leave the canopy, while FPAR is proportional to only the *one-way* penetration and absorption of PAR through the canopy [e^{-kL_T}] The two parameters, a_N and FPAR, will be proportional to each other if Eq (3) is satisfied

If the soil or background material underlying the canopy is relatively dark, so that

$$\frac{\partial a_V}{\partial L_T} \to 0,$$

we can write

$$\frac{\partial (\text{SR})}{\partial L_T} \propto \frac{\partial a_N}{\partial L_T} \tag{4}$$

It follows then that FPAR is proportional to SR

Figure 1a shows how the canopy visible and near-infrared reflectances, a_V and a_N, the simple ratio vegetation index SR, and FPAR vary with leaf area index for the (almost ideal) model canopy described in Table 1 Figure 1b illustrates how the nonlinear functions of leaf area index, SR and FPAR, shown in Figure 1a are almost linearly related to each other because of the relationship expressed in Eq (3)

The analysis summarized above provides a theoretical foundation for the correlation between the SR and FPAR established by empirical analysis of remote sensing data, Eq (3) is normally a reasonable approximation for canopies composed of randomly distributed elements with identical reflectance properties overlying dark soils It is important to note, however, that the system of equations given in Sellers (1987) provides a general basis for relating hemispheric reflectance measurements to canopy, leaf, and soil properties—regardless of whether the above approximation is true

Sellers (1985, 1987) also examined the relationship between canopy reflectance and the use of PAR by leaves for net photosynthesis A_n and the regulation of stomatal conductance g_s This is a more complex problem since these physiological

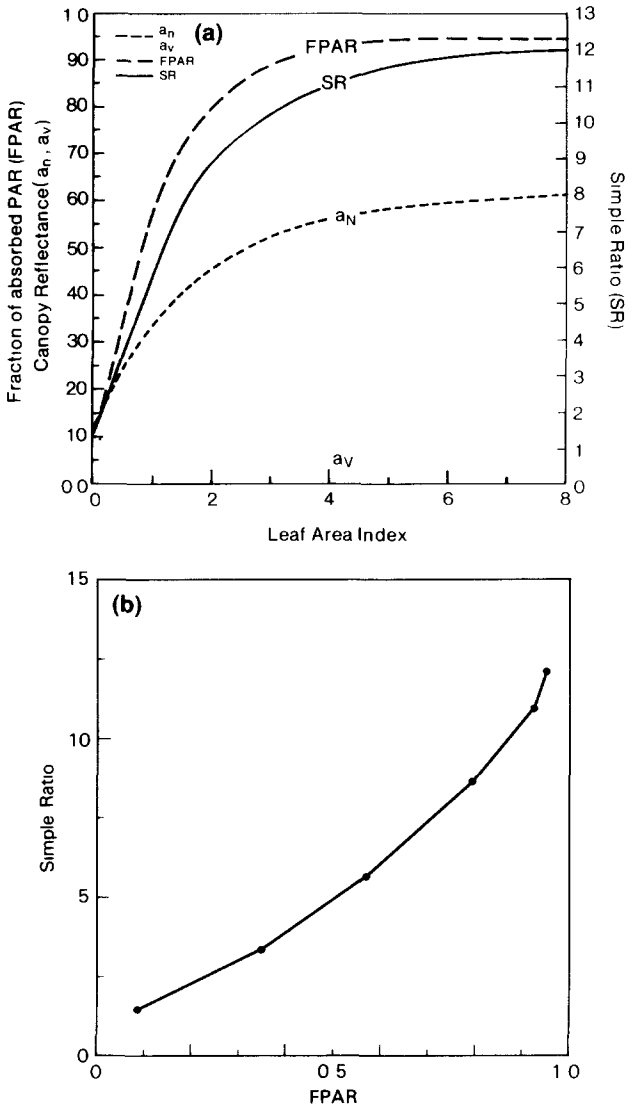

Figure 1 a) Variation of canopy optical parameters with leaf area index as calculated by the two-stream approximation model of Sellers (1985, 1987) with parameters taken from Table 1 a_v, a_N = visible and near infrared (hemispherically-integrated) reflectances, SR = simple ratio vegetation index, FPAR = fraction of PAR absorbed by the canopy b) Simple ratio vegetation index plotted against FPAR, replotted from Figure 1(a) Dots on the curve refer to values of leaf area index, 0 1, 0 5, 1 0, 2 0, 4 0, 8 0, reading from left to right

processes are influenced by several other variables (temperature, water vapor content of the air, water potential of the leaf, and the prior history of the leaves in the canopy) in addition to the absorbed flux of PAR

In the treatment of Sellers (1985, 1987), the models of Charles-Edwards and Ludwig (1974) and Jarvis (1976) were used to describe leaf photosynthesis and leaf stomatal conductance, respectively

$$A_n = \left[\frac{a_1 \mathbf{F}\ \mathbf{n}}{b_1 + \mathbf{F}\ \mathbf{n}}\right] [f(T)f(\varphi_l)f(\delta e)], \quad (5a)$$

$$g_s = \left[\frac{b_2 + \mathbf{F}\ \mathbf{n}}{a_2 + b_2 c_2 + c_2 \mathbf{F}\ \mathbf{n}}\right] [f(T)f(\varphi_l)f(\delta e)], \quad (5b)$$

where

A_n = leaf photosynthesis (μmol m^{-2} s^{-1}) $\equiv P$ in Sellers (1985, 1987),

a_1, b_1 = species-dependent constants (μmol m^{-2} s^{-1}, or W m^{-2}),

$\mathbf{F}$ = (vector) flux of PAR (μmol m^{-2} s^{-2} s^{-1} or W m^{-2}),

$\mathbf{n}$ = vector of leaf normal,

$f(T), f(\varphi_l), f(\delta e)$ = adjustment factors to account for the effects of temperature, leaf water potential, and vapor pressure deficit stress,

g_s = leaf stomatal conductance for water vapor, (mol m^{-2} s^{-1} or m s^{-1}),

a_2, b_2, c_2 = species-dependent constants (mol mol^{-1} or J m^{-3}, mol m^{-2} s^{-1} or W m^{-2}, (mol m^{-2} s^{-1})$^{-1}$ or s m^{-1})

The formulation used in (5b) is consistent with the nomenclature used in Sellers (1985, 1987) It was assumed that all the leaves in the canopy respond identically to $\mathbf{F}\ \mathbf{n}$ The constants a_1, b_1, a_2, b_2, and c_2 can be determined from curve fits to data (see Table 1) The stress factors $f(x)$ vary from unity, under optimal conditions, to zero when photosynthesis and transpiration are totally suppressed by adverse environmental conditions (see Jarvis, 1986, Sellers et al , 1989, Collatz et al , 1991)

The combination of the environmental stress factors was assumed to operate more or less uniformly throughout the canopy so that in estimating canopy photosynthesis and conductance it is only necessary to integrate Eqs (5) with respect to the variation of intercepted PAR, $\mathbf{F}\ \mathbf{n}$, down through the canopy The canopy integral forms of (5) may then be written as

$$A_c = f(\Sigma) \int_0^{L_T} \left[\frac{a_1 \mathbf{F}\cdot\mathbf{n}}{b_1 + \mathbf{F}\ \mathbf{n}}\right] dL, \quad (6a)$$

$$g_c = f(\Sigma) \int_0^{L_T} \left[\frac{b_2 + \mathbf{F}\ \mathbf{n}}{a_2 + b_2 c_2 + C_2\ \mathbf{F}\ \mathbf{n}} \right] dL, \quad (6b)$$

where

A_c = canopy photosynthesis (μmol m^{-2} s^{-1}),
g_c = canopy conductance (mol m^{-2} s^{-1} or m s^{-1}),
$f(\Sigma) = f(T) f(\psi_l) f(\delta e)$

The PAR flux vertical component is assumed to be attenuated as it passes down through the canopy following the semiempirical expression of Goudriaan (1977)

$$F_L = F_0 e^{-kL} \quad (7)$$

where

F_L = PAR flux at leaf area index L in the canopy (μmol m^{-2} s^{-1} or W m^{-2}),
F_0 = PAR flux above the canopy (μmol m^{-2} s^{-1} or W m^{-2}),
L = cumulative leaf area index

Insertion of Eq (7) into (6) allows evaluation of A_c and g_c (see Sellers, 1985, Tables 3 and 4) [Note The combination of (6) and (7) only accounts for the variation of PAR intensity with canopy depth, a mean leaf angle is assumed throughout Sellers (1985) explored the impact of this simplification on the calculation of the bulk canopy properties, A_c and g_c Full integrations over leaf angle and orientation were made prior to the integration with canopy depth, the difference between the results obtained with the full (leaf angles and orientations, canopy depth) and simplified (mean leaf angle / orientation, canopy depth) integrations was found to be practically negligible]

We may now rewrite Eqs (6) as

$$A_c = A_c^* f(\Sigma), \quad (8a)$$

$$g_c = g_c^* f(\Sigma), \quad (8b)$$

where A_c^* and g_c^* are the integrated kernels of (6) and represent the canopy-scale values of the unstressed photosynthetic rate and conductance

Figures 2a and 2b show how A_n, A_c^* and g_s, g_c^* vary with incident PAR flux F_0, according to Eqs (5) and (6) (Here A_n and g_s refer to leaves at the very top of the canopy, fully exposed to the ambient PAR flux F_0)

Figures 2c and 2d show how A_c^* and g_c^* vary with total leaf area index For any given PAR flux, there is a diminishing increase in A_c^* and g_c^* for further increments of leaf area index as more and more of the canopy consists of shaded leaves which have progressively lower rates of A_n and g_s Now an inspection of the solutions to Eqs (6) or (8) [see Tables 3 and 4 in Sellers (1985)] shows that, for low values of the incident PAR flux F_0, the derivatives of A_c^* and g_c^* with respect to total canopy leaf area index L_T are proportional to the derivative of FPAR with L_T and to e^{-kL_T}

$$\frac{\partial A_c^*}{\partial L_T}, \frac{\partial g_c^*}{\partial L_T} \propto e^{-kL_T}, \quad \frac{\partial (\mathrm{FPAR})}{\partial L_T}, \quad \text{as } F_0 \to 0 \quad (9)$$

Equation (9) holds because the PAR flux is used to drive photosynthesis and conductance as it is progressively absorbed through the canopy Figures 2e and 2f show A_c^* and g_c^* plotted against FPAR, and it can be seen that, for the lower values of F_0, Eq (9) holds resonably well This is because, at low values of F_0, all the leaves in the canopy have approximately the same slope of A or g_s against F_0 (see Figs 2a and 2b) At higher values of F_0, however, the leaves at the top of the canopy are saturated (no change in A or g_s with F_0), but the leaves lower down are still below saturation, resulting in an increasingly nonlinear relationship between A_c^*, g_c^*, and FPAR with increasing F_0 This effect can be seen more clearly in Figures 2g and 2h, where A_c^*/F_0 and g_c^*/F_0 are plotted against FPAR The lines corresponding to the lowest values of F_0 are the most nearly linear, degrading to more nonlinear forms as F_0 increases

Comparing Eqs (2), (4), and (9), we have the chain of relationships

$$\frac{\partial A_c^*}{\partial L_T}, \frac{\partial g_c^*}{\partial L_T} \propto \frac{\partial (\mathrm{FPAR})}{\partial L_T} \propto \frac{\partial a_N}{\partial L_T} \propto \frac{\partial (\mathrm{SR})}{\partial L_T}, \quad \text{as } F_0 \to 0 \quad (10)$$

so that under the specified conditions—uniform canopy, dark underlying soil, low levels of F_0—A_c^* and g_c^* should be proportional to SR and other SVI However, on clear days F_0 values typically reach 200–400 W m^{-2} and so this approximation should be viewed with some caution Additionally, further nonlinear effects are induced when the vegetation within the field of view is clumped into spatially heterogenous units (see Fig 21 of Sellers (1985)]

This apparent nonlinearity of canopy function potentially degrades the prospects for realistic estimation of CO_2 assimilation using remote sens-

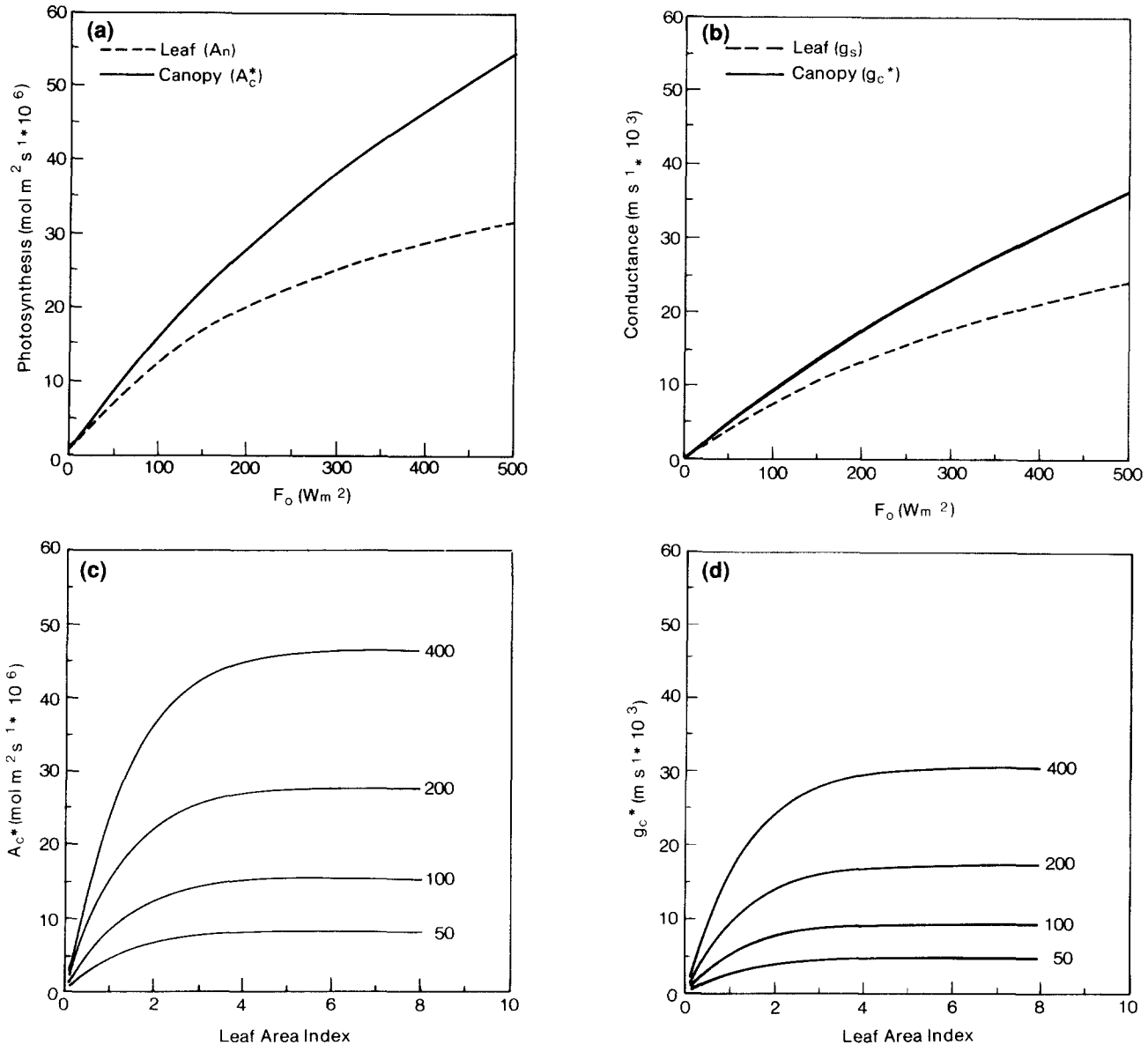

Figure 2 a,b) Unstressed leaf, A_n and g_s, and canopy, (A_c^* and g_c^*), photosynthesis and conductance as functions of incident PAR flux, F_0, calculated using Eqs (5) and (6) in text, parameters from Table 1 Total leaf area index for the canopy, $L_T = 8$ c,d) Variation of unstressed canopy photosynthesis, A_c^*, and conductance, g_c^*, with leaf area index and PAR flux, F_0, calculated using Eqs (6) Values of F_0 are marked on the curves

ing It results from the fact that, in the formulation of Sellers (1985, 1987), leaves at different levels in the canopy are saturating with respect to **F n** at different levels of F_0 If photosynthetic capacity, as represented by the values of a_1 and b_1 in (5), is constant throughout the canopy, leaves near the top of the canopy would usually be completely light-saturated while leaves near the base would still be on the linear portion of the light-response curve and thus unsaturated This formulation certainly exaggerates any nonlinearity that occurs in nature, because leaves in shaded habits tend to have lower photosynthetic capacities and saturate at lower light levels (Bjorkman, 1981)

In the following sections, we extend the analysis of Sellers (1985) by replacing the empirical leaf models with more general, semimechanistic models of photosynthesis and stomatal conductance In contrast to the uniform distribution of canopy properties with depth assumed above, we explore depth distributions of photosynthetic capacity and maximum stomatal conductance that

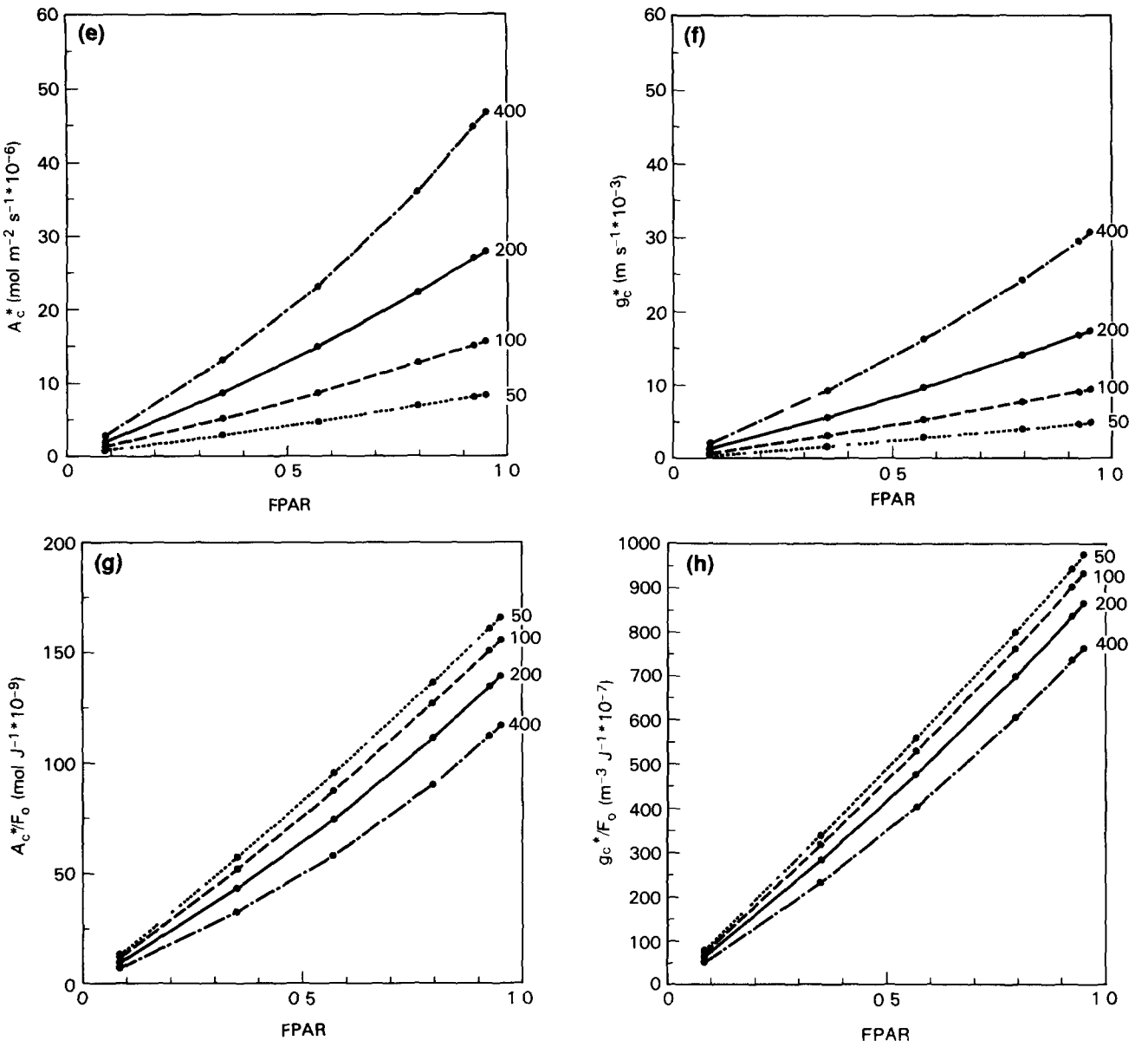

Figure 2 (continued) e,f) Relationships between A_c^*, g_c^*, and FPAR for a range of PAR fluxes using Eqs (6) and the two-stream approximation model described in Sellers (1985, 1987) g,h) Relationship between A_c^* / F_0, g_c^* / F_0 and FPAR, A_c^* / F_0 and g_c^* / F_0 can be considered as surrogates for $\partial A_c^* / \partial F_0$ and $\partial g_c^* / \partial F_0$ The points on the curves refer to values of $L_T = 0.1, 0.5, 1.0, 2.0, 4.0, 8.0$, working from left to right The numbers on each curve refer to values of F_0 in W m^{-2} The canopy is assumed to be uniform and green, overlying a dark background Parameter values are given in Table 1, $f(\Sigma) = 1$

parallel the depth distribution of photosynthetically active radiation. This arrangement is supported by both an expanding base of empirical data and a number of theoretical assessments that identify an optimum depth distribution of photosynthetic capacity for maximizing canopy photosynthesis The results of this analysis are simpler and more general than those from the previous studies, and indicate that the relationships among SR, FPAR, A_C, and g_C should be almost independent of the spatial distribution of the vegetation

Improved Leaf Physiological Models

Farquhar et al (1980) presented a biochemical model of leaf photosynthesis (including photorespiration), subsequently extended by von Caem-

merer and Farquhar (1985) and other researchers, which describes CO_2 assimilation, A, as rate-limited by enzyme kinetics, specifically the amount and cycle time of the carboxylating enzyme Rubisco, and electron transport, which is a function of incident PAR and the efficiency of the leaf's light-intercepting apparatus (chlorophyll) In a recent version of the model (Collatz et al , 1991), A is given by $A = \min(w_c, w_e, w_s)$, where w_c, w_e, w_s are functions which desribe the assimilation rates as limited by the efficiency of the photosynthetic enzyme system, the amount of PAR captured by the leaf chlorophyll and the capacity of the leaf to export or utilize the products of photosynthesis, respectively

The ribulose-bisphosphate (RuBP) carboxylase-oxygenase enzyme (Rubisco) limiting rate on assimilation, w_c, is given by

$$w_c = V_m\left[\frac{C_i - \Gamma^*}{C_i + K_c(1 + O_2/K_o)}\right] \qquad (11)$$

where

w_c = Rubisco-limited rate of assimilation (μmol m^{-2} s^{-1}),
V_m = maximum catalytic capacity of Rubisco (μmol m^{-2} s^{-1})
C_i = concentration of CO_2 in leaf interior (Pa),
O_2 = partial pressure O_2 in leaf interior (Pa),
Γ^* = CO_2 compensation point (Pa),
K_c = Michaelis–Menten constant for CO_2, (Pa),
K_o = inhibition constant for O_2 (Pa)

V_m is given by the product of V_{max} and a temperature-dependent function [see Appendix of Collatz et al (1991) and Table 2] V_{max} is a property of the leaf (or chloroplast) and is proportional to the Rubisco reserves of the leaf (or chloroplast) and thus its nitrogen content Γ^*, K_c, and K_o are all functions of temperature [see Appendix of Collatz et al (1991) and Table 2 of this article]

The light-limited rate of assimilation, w_e, is given by

$$w_c = (\mathbf{F}\ \mathbf{n})\varepsilon(1 - \omega_s)\left[\frac{C_i - \Gamma^*}{C_i + 2\Gamma^*}\right] \qquad (12)$$

where

w_c = light-limited rate of assimilation (μmol m^{-2} s^{-1}),
ε = intrinsic quantum efficiency for CO_2 uptake, (μmol μmol^{-1} or μmol J^{-1})

A third limiting rate has been defined by Collatz et al (1991) w_s is the capacity for the export or utilization of the products of photosynthesis and is estimated by Collatz et al (1991) to be

$$w_s = V_m/2 \qquad (13)$$

The simplest way to proceed is to assume that the assimilation rate is the minimum of w_c, w_e, and w_s (cf Farquhar et al , 1980) However, observations indicate that the transition from one limiting rate to another is not instantaneous and that coupling between the three processes leads to smooth curves rather than superpositioning of straight lines Collatz et al (1991) describe this effect by combining the rate terms into two quadratic equations, which are then solved for their smaller roots

$$\theta w_p^2 - w_p(w_c + w_e) + w_c w_e = 0, \qquad (14a)$$

$$\beta A^2 - A(w_p + w_s) + w_p w_s = 0, \qquad (14b)$$

where

A = assimilation rate (μmol m^{-2} s^{-1}),
θ,β = coupling coefficients,
w_p = "smoothed" minimum of w_c and w_e (μmol m^{-2} s^{-1})

The coefficients θ and β can theoretically range from 1 (no coupling effects) to 0 In nature, these coefficients assume values on the order of 0 8 to 0 99 (see Collatz et al , 1990) Figure 6a shows an example of a sharp transition from w_e to w_c (θ, $\beta = 1$), Figure 6e shows a more gradual transition (θ, $\beta = 0\ 8$)

Net assimilation A_n is then given by

$$A_n = A - R_d, \qquad (15)$$

where

R_d = leaf respiration rate (μmol m^{-2} s^{-1})

Collatz et al (1991) scaled R_d to the leaf carboxylase content by

$$R_d = 0\ 015V_m \qquad (16)$$

Table 2 Forcing Variables, Leaf Parameters, and Derived Output Variables for the Coupled Stomatal-Photosynthesis Leaf Physiology Models

Symbol	*Variable*	*Values*	*Units*
	A Forcing Variables		
C_a	CO_2 concentration in CAS†	34	Pa
F_0	PAR flux above canopy	50, 100, 200, 400 230, 460, 920, 1840	W m^{-2} μmol m^{-2} s^{-1}
g_b	Leaf boundary layer conductance (H_2O)	0 04	m s^{-1}
h_a	Relative humidity of CAS	0 1, 0 25, 0 5, 0 75	
O_2	O_2 concentration in CAS†	20,900	Pa
p	Atmospheric pressure†	$1\,013 \times 10^5$	Pa
T_s	Leaf temperature	310	K
μ	Cosine of incident angle of PAR flux	0 25, 0 5, 0 75, 1 0	
	B Leaf Parameters		
b	Minimum stomatal conductance†	0 01	mol m^{-2} s^{-1}
$G(\mu)$	Leaf angle distribution function (replaces n)	0 5	–
K_c	Michaelis–Menten coefficient for CO_2†	$30*2\,1^{Q_t}$	Pa
K_o	Inhibition coefficient for O_2†	$30{,}000*1\,2^{Q_t}$	Pa
L_T	Total leaf area index	0 1, 0 5, 1 0, 2 0, 4 0, 8 0	m^2 m^{-2}
m	Slope parameter†	9 0	–
Q_t	Q_{10} temperature coefficient†	$(T_s - 298)/10$	–
S	CO_2 / O_2 specificity†	$2600*0\,57^{Q_t}$	–
V_m	Maximum leaf catalytic capacity at T_s	$V_{max}*2^{Q_t}$	μmol m^{-2} s^{-1}
V_{max}	Maximum leaf catalytic capacity at 298 K	200	μmol m^{-2} s^{-1}
V_{max_0}	V_{max} for top leaves†	200	μmol m^{-2} s^{-1}
Γ^*	CO_2 photocompensation point†	O_2 / (2S)	Pa
ε	Quantum efficiency for CO_2 uptake†	0 08	mol mol^{-1}
ω_0	Leaf scattering coefficient for PAR	0 2	–
θ, β	"Linkage" coefficients between w_e, w_c, w_s	1 0, 1 0, 0 8, 0 8	–
	C Derived Variables		
A	Assimilation rate	–	μmol m^{-2} s^{-1}
C_i	Leaf interior CO_2 concentration	–	Pa
C_s	Leaf surface CO_2 concentration	–	Pa
E	Transpiration rate	–	mol m^{-2} s^{-1} or m s^{-1}
g_s	Leaf stomatal conductance (H_2O)	–	mol m^{-2} s^{-1} or m s^{-1}
h_s	Leaf surface specific humidity	–	–
R_d	Respiration rate	–	μmol m^{-2} s^{-1}

[a] Values of forcing variables and leaf parameters used to test integration schemes were taken from Collatz et al (1991) when indicated by † CAS stands for canopy air space

Collatz et al (1991) went on to incorporate the above photosynthesis model with the Ball (1988) semiempirical model for leaf stomatal resistance

$$g_s = m\frac{A_n}{C_s}h_s p + b, \qquad (17)$$

where

g_s = stomatal conductance for water vapor (mol m^{-2} s^{-1} or m s^{-1}),
m = coefficient from observations $\simeq$ 9 for C_3 plants,
b = coefficient from observations $\simeq$ 0 01 for C_3 plants (mol m^{-2} s^{-1} or m s^{-1}),
h_s = relative humidity at leaf surface,
C_s = CO_2 concentration at leaf surface (Pa),
p = atmospheric pressure (Pa),
p_s = standard atmospheric pressure $= 1\,013 \times 10^5$ (Pa),
T_f = freezing temperature = 273 16 K,

$$g_s \text{ (m s}^{-1}) = 0\,0244\frac{T}{T_f}\frac{p_s}{p}g_s \text{ (mol m}^{-2}\text{ s}^{-1})$$

The leaf surface environment variables, h_s and C_s, are given by (see Fig 3)

$$(H_s - H_a)g_b = (H_i - H_s)g_s = E \qquad (18a)$$

We also see from Figure 3 that

$$h_s = \left[\frac{H_s}{H_i}\right], \qquad (18b)$$

$$\frac{(C_a - C_s)}{p}\frac{g_b}{1.4} = \frac{(C_s - C_i)}{p}\frac{g_s}{1.6} = A_n, \qquad (18c)$$

where

H_a, H_s, H_i = water vapor concentration in the external air, at the leaf surface and inside the leaf, respectively (mol mol^{-1}),

g_b = leaf boundary layer conductance for water vapor (mol m^{-2} s^{-1} or m s^{-1}),

E = transpiration rate (mol m^{-2} s^{-1} or m s^{-1}),

C_a, C_s = carbon dioxide concentration in the external air and at the leaf surface, respectively (Pa),

1.4, 1.6 = factors to account for different diffusivities of H_2O and CO_2 in the leaf boundary layer and stomatal pores, respectively

The system is then closed by calculating the CO_2 concentration of the leaf interior

$$C_i = C_s - \frac{1.6A_n}{g_g}p \qquad (19)$$

Figure 3 Coupled stomatal-photosynthesis models as described by Collatz et al (1991) for canopy photosynthesis and transpiration System shows pathways for heat, CO_2 and water vapor flux

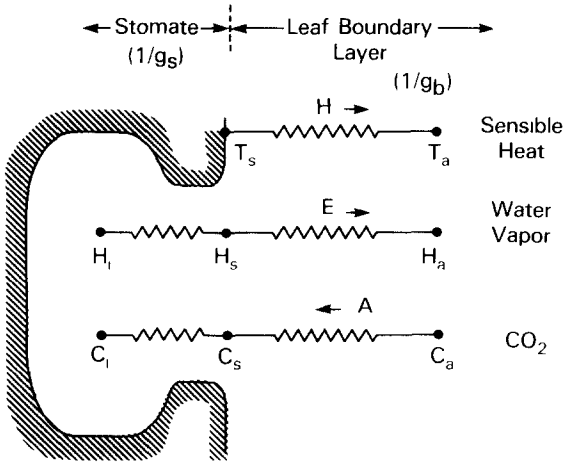

Figure 3 shows how the fluxes of water vapor, temperature, and heat from a leaf to the external air are assumed to behave in this model Figure 4 shows how the system of equations is solved in practice Table 2 lists the required forcing variables (environmental conditions), leaf parameters, and the derived (output) variables given by the solution of the equation set described in this section and depicted in Figure 4

The Scaling of Leaf Physiology to Canopy Position

Leaves in shaded microsites have lower photosynthetic capacities and maximum stomatal conductances than leaves in exposed microsites (Bjorkman, 1981) This extremely general pattern applies to plants grown in controlled environments with high and low light (Bjorkman and Holmgren, 1963, Evans, 1989a), to lower and upper leaves on a single plant (Field, 1983, Hirose and Werger, 1987), and to mixed species assemblages with shade-tolerant understory species beneath a canopy of different species (Bazzaz, 1979, Schimel et al , 1991) Species differ greatly in their phenotypic plasticity (Seemann et al , 1987,

Figure 4 Iterative solution method for the photosynthesis-stomatal conductance model, after Collatz et al (1991) equation set

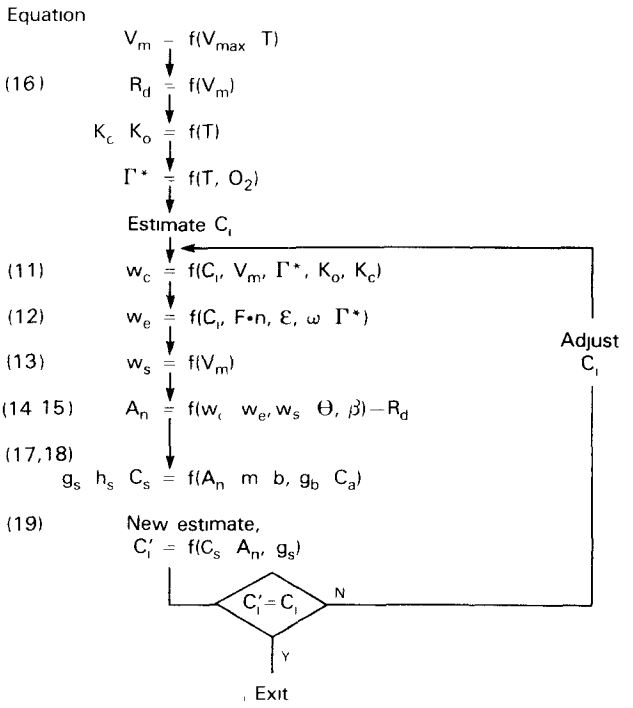

Evans, 1989a), in response to growth in low or high-light habitats (Bjorkman and Holmgren, 1963), and in the extent to which stress factors other than light depress photosynthetic capacity (Mooney, 1972) All of this intrinsic complexity is the raw material from which ecological and evolutionary factors shape plant canopies, with the result that the depth-distribution of photosynthetic capacity in real canopies tends to be quite predictable

Why does the shaping of plant canopies of ecological and evolutionary factors constrain the response of photosynthetic capacity to light availability? Three factors appear to be critical First, the basic mechanisms of photosynthesis are essentially identical in all C_3 plants (more than 85% of all plant species), and differences in capacity are largely driven by differences in investment in the biochemical machinery of photosynthesis The strong, linear relationship between photosynthetic capacity and leaf nitrogen (Field and Mooney, 1986, Evans, 1989b) attests to this linkage between investment and capacity Second, the investments required to support photosynthesis are expensive Nitrogen nutrition alone can consume from 20% to 45% of the carbon fixed in photosynthesis (Chapin et al , 1987) Third, any plant that invests too much photosynthetic capacity in any leaf should be at a competitive disadvantage to a plant that matches investments to local resource (especially light) availability For a single plant with leaves distributed through a canopy, the criterion for the most efficient distribution of capacity is given by the solution to the isoperimetric problem in dynamic control theory (see Intriligator, 1971, Bloom et al , 1985) Specifically, if photosynthetic capacity is limited by some quantity Z that is expensive for the plant to acquire, then the returns on any fixed investment in Z are greatest when

$$\frac{\partial A_{\text{int}}}{\partial Z} = \lambda, \tag{20}$$

where A_{int} is photosynthesis integrated over an appropriate spatial or temporal scale and λ is an undefined Lagrangian multiplier In the analyses to date, Z has been considered as transpiration in a single leaf (Cowan and Farquhar, 1977), leaf nitrogen in a canopy (Field, 1983), leaf mass in a canopy (Gutschick and Wiegel, 1988), and photosynthetic capacity in a leaf (Farquhar, 1989) A_{int} is typically the instantaneous value of photosynthesis for single leaf analyses but the single-leaf daily integral for canopy analyses If the condition in Eq (20) holds for instantaneous values, it also holds for daily integrals The problem of optimal resource allocation has no general solution when a canopy is composed of many plants or species, but the single plant solution may be approximately correct, as long as all plants tap a common pool of below-ground resources and construct tissues of similar composition and cost

PAR is also expensive to acquire, because plants cannot capture it without investing in leaves, stems, and branches Formally, the problem is identical to those already solved As long as

$$\frac{\partial^2 A}{\partial[(\mathbf{F}\cdot\mathbf{n})(1-\omega_v)]^2} < 0 \tag{21}$$

for all A, then we can also write

$$\frac{\partial A}{\partial[(\mathbf{F}\cdot\mathbf{n})(1-\omega_v)]} = \lambda_1, \tag{22a}$$

which leads to

$$\frac{\partial A_c}{\partial(\text{FPAR})} = \lambda_2, \tag{22b}$$

where the value of λ is different for each quantity (water, nitrogen, mass, or PAR) and also depends on the level of each quantity invested as well as on the status of the environmental variables that influence photosynthesis and transpiration

Equation (22) implies that, at all levels in the canopy, leaves begin to saturate with respect to $(\mathbf{F}\ \mathbf{n})(1-\omega_v)$ at the same F_0 In fact, the light response curves for leaves at all levels of the canopy should be scaled versions of a single response, with a scaling factor proportional to $[(\mathbf{F}\ \mathbf{n})(1-\omega_v)]/F_0$ As long as dark respiration is the same at all levels in the canopy or is proportional to $V_{\max}$ [as in this analysis, see Eq (16)], then the light saturated photosynthetic rate, or $A_{\max}$, should also be proportional to $[(\mathbf{F}\ \mathbf{n})(1-\omega_v)]/F_0$ or to $(\mathbf{F}\ \mathbf{n})(1-\omega_v)$

At any level in the canopy, the value of $[(\mathbf{F}\ \mathbf{n})(1-\omega_v)]/F_0$ changes during the day, on a time scale that changes in $A_{\max}$ are unlikely to track Again, for optimum efficiency, adjustments in $A_{\max}$ are likely to follow a moving time average of the light regime An expanding body of empirical data, including the results of Field (1983),

Walters and Field (1987), and Pons et al (1990), directly supports the prediction that A_{max} for each leaf should be proportional to the time-averaged or integrated PAR that that leaf experiences Additional studies, including DeJong and Doyle (1985), Hirose and Werger (1987), Hirose et al (1989), Kittel et al (1990), and Schimel et al (1991), reported that leaf nitrogen, a strong correlate of A_{max}, parallels integrated PAR These studies extend the generality of the relationship, because they involve a multispecies prairie (Schimel et al , 1991) and single-species swards in which the leaf-age gradient places the youngest leaves at either the top of the canopy (Hirose and Werger, 1987) or the bottom (Hirose et al , 1989) Over a broad range of species and ecosystems, and with few exceptions (e g , Leverenz and Jarvis, 1980), the general pattern matches the prediction from theory—A_{max} and leaf nitrogen [N]—should scale with the time-integral of the absorbed local PAR

These arguments and Eq (22) suggest that the profile of leaf nitrogen, [N], and V_{max} down through the canopy should follow some time average of the PAR flux, most likely the radiation-weighted, time-mean $\bar{\mathbf{F}}$ However, while this paradigm describes the relative distribution of [N], it does not say anything about the absolute values of [N] and V_{max} within the canopy, which are more likely to be constrained by the overall availability of nutrients within the plants environment For optimal efficiency, canopies can be expected to allocate [N] such that for a specified light regime ($\mathbf{F}$ n) operating over a period T on the order of several days to a few weeks

$$U_1 \int_0^T A \, dt + U_2 \int_0^T \frac{A}{[N]} \, dt, \qquad (23)$$

is maximized for all L

U_1 and U_2 are cost-benefit weighting factors which would be largely determined by the local availability of nitrogen In a nitrogen-rich environment, where there is little cost in maintaining high values of V_{max}, U_1 should be much greater than U_2 and so maximizing photosynthesis [first term in Eq (23)] would have a higher priority than maximizing efficiency [second term in Eq (23)] Conversely, in nutrient-poor environments, we can expect U_2 to be greater than U_1 Whatever the conditions, the value of V_{max} arrived at from (23) can be associated with a reference value of PAR flux, $\tilde{\mathbf{F}}$, which light-saturates the leaves, that is, $\tilde{\mathbf{F}} = \mathbf{F}$ when $w_i = w_c$ Under most conditions, when $U_1 >> U_2$, this reference value of $\tilde{\mathbf{F}}$ would be close to, if not equal to, the radiation-weighted time-mean value of $\mathbf{F}$, $\bar{\mathbf{F}}$, for smoothly varying fluxes for simplicity, we shall assume that $\tilde{\mathbf{F}} \simeq \bar{\mathbf{F}}$ from now on

INTEGRATING THE COUPLED LEAF STOMATAL–PHOTOSYNTHESIS MODEL OVER THE CANOPY

From the analysis and observations discussed in the previous section, we propose that the profiles of leaf nitrogen, [N], V_{max}, and hence V_m within the plant canopy are distributed according to the radiation-weighted time-mean profile of PAR

$$V_m = V_{m0}\overline{f(L)} \qquad (24a)$$

where

V_{m0} = maximum, that is, "top" leaf, value of V_m in the canopy (μmol m^{-2} s^{-1})
= product of V_{max0} and a temperature inhibition function (see Table 2),

$\overline{f(L)}$ = time-averaged variation of PAR flux with LAI [e g , e^{-kL} Eq (7)]

Also, for most conditions where nutrients are not in drastically short supply, that is, $U_1 >> U_2$ in Eq (23), the value of V_{m0} will be determined by the radiation-weighted time-mean flux of PAR, $\bar{F}_0$, at the top of the canopy, that is,

$$V_{m0} = \text{function of } (w_c = w_l) \quad \text{when } \mathbf{F}_0 = \bar{\mathbf{F}}_0 \qquad (24b)$$

To obtain V_{m0} as defined in (24b), $\mathbf{F}_0$ is inserted into (12) and the derived value of w_c used in place of w_c in (11) to calculate V_m (in this case V_{m0})

The overbar on $f(L)$ in (24a) denotes "radiation-weighted time-mean value" Using the example of Eq (7) to describe $f(L)$, we then have

$$\overline{f(L)} = e^{-\bar{k}L}, \qquad (25a)$$

$$\bar{\mathbf{F}} = \bar{\mathbf{F}}_0\overline{f(L)}, \qquad (25b)$$

$$\bar{k} = [G(\mu)/\mu](1 - w_c)^{1/2} \qquad (25c)$$

Note that Eq (25) also implies a time-mean zenith angle $\bar{\mu}$ for the flux $\bar{\mathbf{F}}$

The instantaneous light-limited value of photosynthesis, w_e, is given by Eq (12) A full treatment of canopy photosynthesis would take into

account the entire range of leaf angles and orientations at every level on the canopy in addition to carrying out the top-to-bottom integration (PAR attenuation as described by Eq (7)), in other words, the **F n** term would be subjected to full azimuth and zenith integrations However, as discussed in Sellers (1985), the adoption of a single mean leaf projection $G(\mu)$ in place of **n** gives very similar results numerically The expression (**F n**) in (12) can therefore be replaced by a simpler function

$$\mathbf{F}\cdot\mathbf{n} = F\frac{G(\mu)}{\mu}$$

$$= F_0\frac{G(\mu)}{\mu}f(L) \qquad (26)$$

We can now construct a canopy-scale model of photosynthesis Equation (24) is combined with Eq (11) to give an expression for the variation of w_c with canopy depth

$$w_c = a_0\overline{f(L)}, \quad a_0 = V_{m0}\left[\frac{C_i - \Gamma^*}{C_i + K_c(1 + O_2/K_o)}\right] \qquad (27a)$$

where

V_{m0} = mean value of V_m for the ensemble of leaves at the top of the canopy (μmol m^{-2} s^{-1})

Equation (26) is combined with (12) to give an equivalent expression for w_e

$$w_e = b_0 f(L), \quad b_0 = \left(\mathbf{F}_0\frac{G(\mu)}{\mu}\right)\varepsilon(1 - \omega_v)\left[\frac{C_i - \Gamma^*}{C_i + 2\Gamma^*}\right] \qquad (27b)$$

The $f(L)$ terms in (27a) and (27b) are different

1. In (27a), the profile of V_m within the canopy is given by the product of V_m at the top of the canopy, V_{m0}, and the radiation-weighted *time-mean* profile of PAR flux down through the canopy, $\overline{f(L)}$ [V_{m0} is related to $\overline{\mathbf{F}_0}$, the reference or *time-mean* (overbar) PAR flux as given by (24a)]
2. In (27b), w_e varies with $f(L)$, the *instantaneous* (no overbar) attenuation function for PAR down through a canopy, and $\mathbf{F}_0$, both of which vary with solar angle and cloud conditions

In reality, leaves within a canopy are subject to variations in leaf surface relative humidity (h_s), leaf surface CO_2 concentration (C_s), boundary layer conductance (g_b), leaf temperature (T_s) and a profile of temperature (T_a), water vapor concentration (H_a), and carbon dioxide concentration (C_a) in the canopy air space The resulting resistance network for this "real" situation is shown in Figure 5a Complete integration of Eq (27) over a canopy is fairly complex, requiring a numerically solved multilayer model of the type described in Sellers and Lockwood (1981) or Goudriaan (1977) In most cases, however, it can be assumed that variations in leaf temperature (T_s) and the canopy air space profile gradients of T_a, H_a, and C_a are small so that the resistance network can be simplified to that shown in Figure 5b, where T_s, T_a, e_a, and C_a are assumed to be invariant with depth Sensitivity studies by Sellers and Lockwood (1981) indicated that, for the case of modeled transpiration from dry canopies, the difference between results produced by the integration schemes represented by Figures 5a and 5b is relatively small

Following Figure 5b, the solution of the equation set for the entire canopy is now a relatively simple matter of numerical integration, more or less following the procedure used in Figure 4 Typical values of the forcing variables and leaf parameters listed in Table 2 were extracted from Collatz et al (1991) to construct a model copy It will be remembered that V_m is given by the product of a leaf physiological property, V_{max}, and a temperature function (see Table 2) In this case, the value of V_{max0} was taken to be equal to the value of V_{max} in Collatz et al (1991) and the profile of V_{max} was given by Eq (24) For this worked example $\bar{\mu}$, $G(\bar{\mu}) = 0\,5$ This corresponds to a canopy of spherically distributed leaves exposed to a time-mean flux of F_0 with direction of $\bar{\mu} = 0\,5$ (solar zenith angle = 60°) In Table 2, the quantum efficiency coefficient ε is assumed to be constant with canopy depth, following the observations of Ehleringer and Bjorkman (1977) A maximum leaf area index L_T of 8 was chosen for the study which represents a near maximum for normal broad-leaf conditions and provides a severe test of the integration schemes over the depth-varying PAR regime In this and all subsequent calculations, the vegetation is assumed to be free of soil moisture stress

Figure 6 shows the light response curves for leaves at different levels in the model canopy note in Figures 6c and 6d how the leaves all

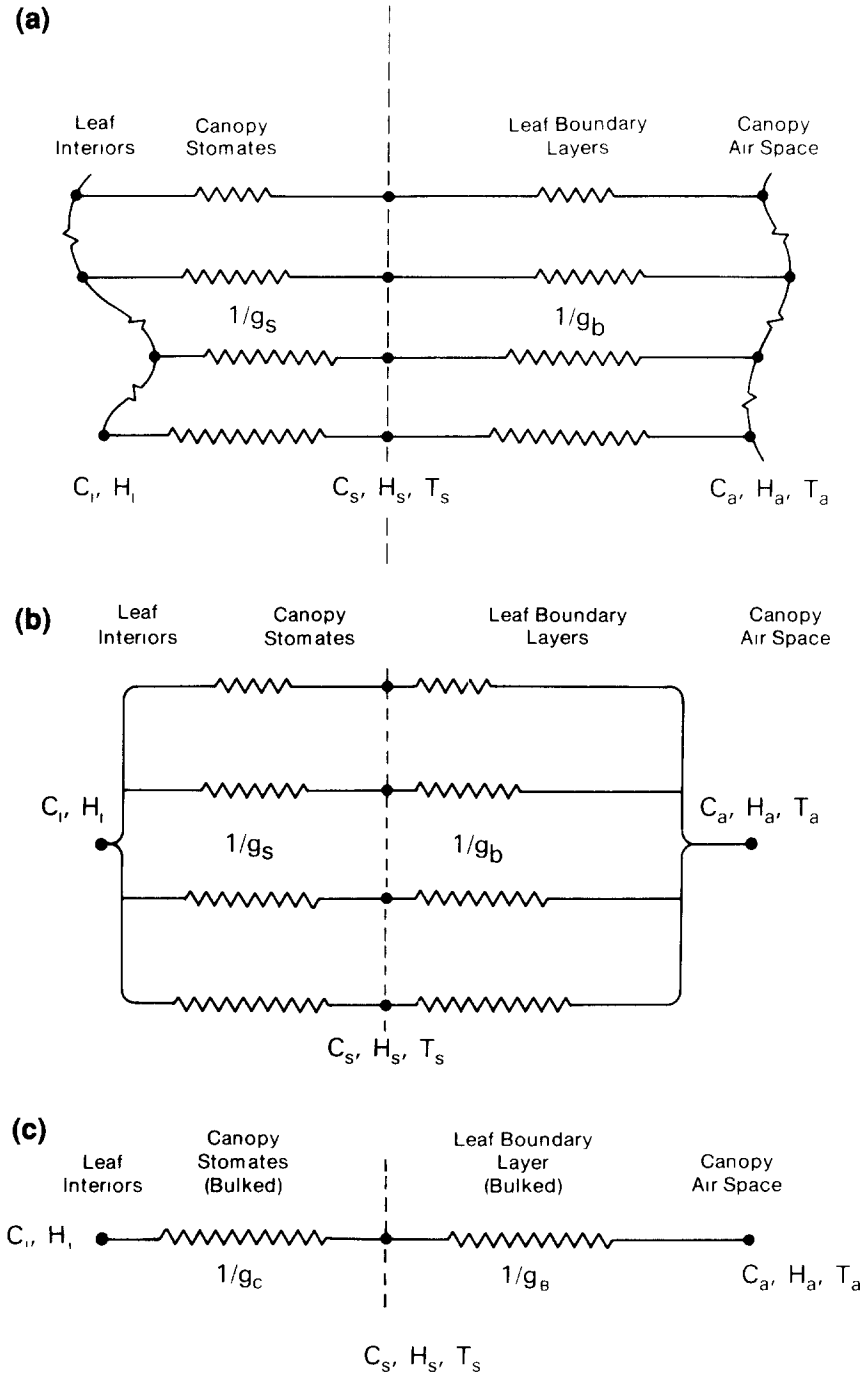

Figure 5 Resistance network corresponding to different canopy integration schemes a) Full scheme with developed profiles of T_a, H_a, C_a, and T_s b) Restricted numerical scheme with T_a, H_a, C_a, and T_s invariant with canopy depth c) Bulk (semianalytical) scheme with T_a, H_a, C_a, and T_s invariant with depth and bulk values of C_i, H_s, and C_s In a) and b), **F** has direction μ, where μ is not necessarily $\bar{\mu}$ In c), $\mu = \bar{\mu}$

saturate at one value of $\mathbf{F}_0$, thus satisfying Eq (22) [The curves for the uppermost leaves in Figures 6e and 6f (θ, $\beta = 0$ 8) were used to fit Eqs (5) and derive the parameters a_1, b_1, a_2, b_2, and c_2 listed in Table 1 and used in Fig 2]

Figures 7a–f show some results from simulations based on numerically integrating (27) over the canopy—80 layers were used Note how the behavior of the complete canopy follows that of the top leaves when $h_s \rightarrow 1$ (compare Figs 6 and 7) Figure 8 shows how various biophysical states and rates can vary with depth in the model canopy the profiles of C_i, h_s, g_s, and A are fairly well developed In Figure 9, the effect of PAR intensity and incidence angle is shown, except for the extreme and physically implausible cause of high

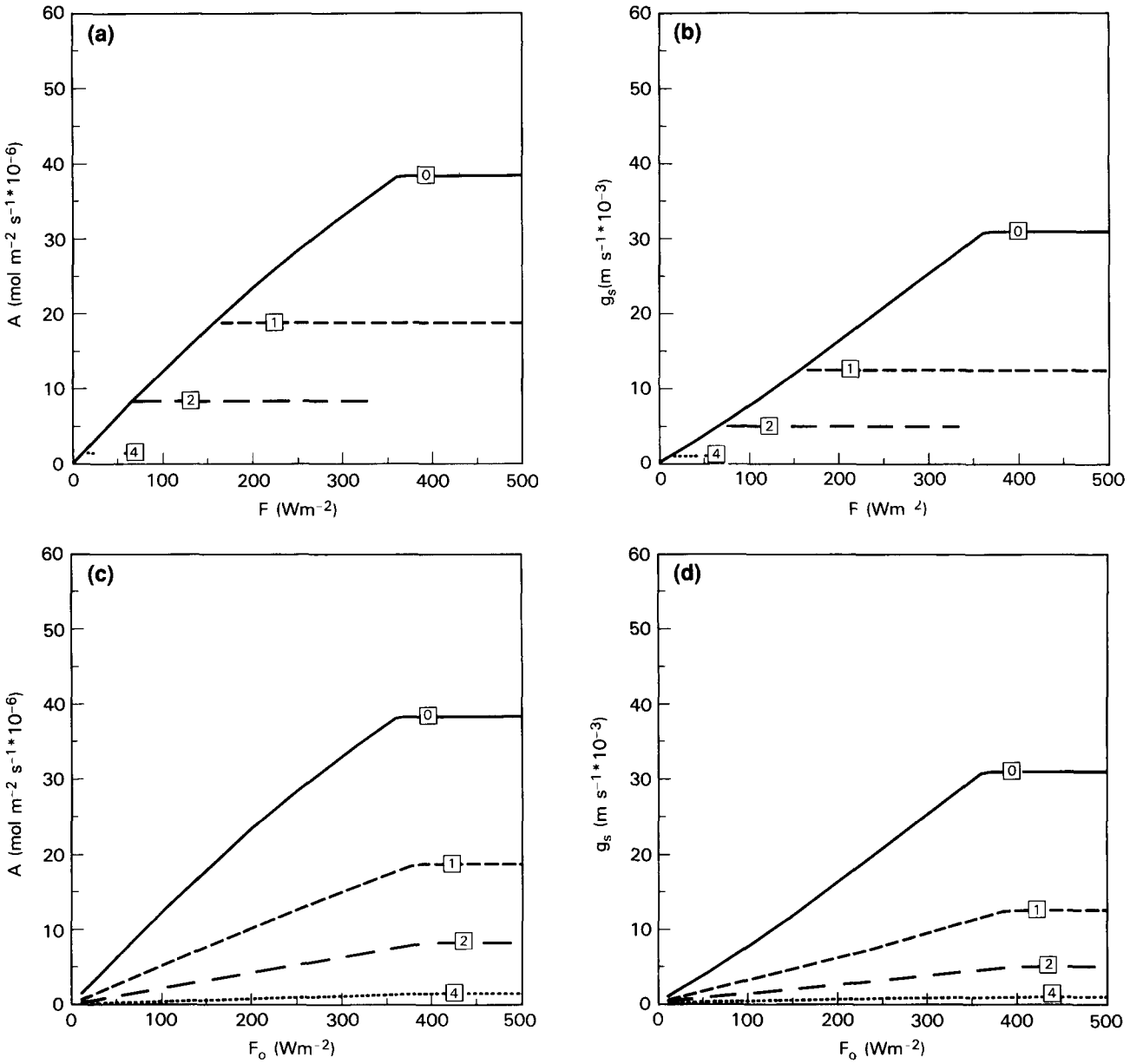

Figure 6 Dependence of leaf photosynthesis and leaf conductance on PAR as calculated using the coupled stomatal–photosynthesis model (Fig 4) In all cases, relative humidity in the canopy air space was held at unity, $h_s \rightarrow 1$, and leaf respiration R_d was set to zero The numbers in boxes refer to leaf position in terms of cumulative leaf area index a,b) A and g_s versus the mean value of incident, PAR, F, for leaves at different depths in the canopy, $L = 0$ refers to "top" leaves θ, $\beta = 1\ 0$ c,d) Same as a) and b) except that all leaf responses are plotted against F_0, note how all leaves saturate at roughly the same value of F_0 $\theta, \beta = 1\ 0$

PAR fluxes at glancing angles (i e , to the left of the numerical solution maxima), the canopy process rates show little variation with μ

Figure 10 explores the effects of varying g_b within the canopy Three depth dependences of g_b are used g_b is assumed to be invariant with depth ($g_b = 0\ 04$ m s^{-1}), g_b varies linearly with depth, and g_b varies exponentially with depth, more or less as in the Simple Biosphere Model (SiB) of Sellers et al (1986) In all three cases, the integral of g_b over the depth of the canopy is the same, 0 32 m s^{-1} It appears that variations in the profile form of g_b have some influence on the estimate of canopy-integrated conductance g_c and E_c (In

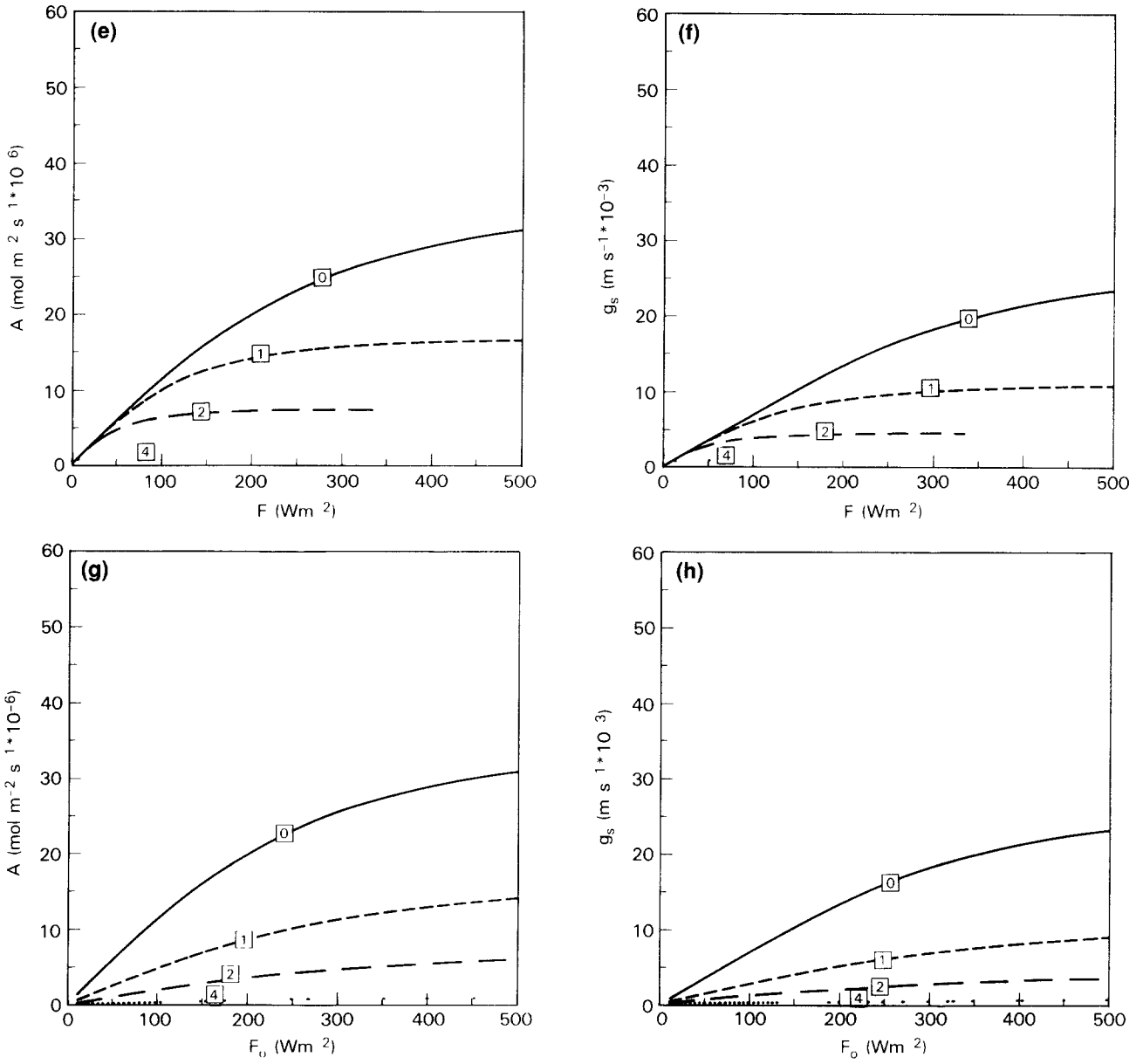

Figure 6 (continued) e,f) Same as a) and b) except θ, $\beta = 0.8$ The top leaf", $L = 0$, responses were used to fit Eq (5) and derive values of a_1, b_1, a_2, b_2, and c_2, see Table 1 g,h) Same as c) and d) except θ, $\beta = 0.8$

these figures and all subsequent equations, the use of a capital subscript refers to a bulk or canopy-integrated quantity)

The solutions shown in Figures 7–10 for the numerical integration scheme of Figure 5b were used to evaluate the accuracy of a simpler bulk integration scheme suitable for operational applications

Figure 5c shows the bulk integration scheme for the canopy Essentially, bulk or integral values of C_i, g_s, and g_b (C_i, g_c, g_a) are specified which in turn implies bulk values of C_s, h_s, A, and E The canopy transfers of CO_2 and H_2O are thus treated as bulk integrated fluxes as in SiB It is further assumed that $\mu \simeq \bar{\mu}$, so that $f(L)$ is replaced by $\overline{f(L)}$ in Eq (27b) The PAR and V_{max} extinction terms are now identical [both are defined by $\overline{f(L)}$] so the canopy-depth portion of the integral can be separated from the physiological portion of the equation set Equation (27) can then be substituted into Eq (14a) and solved to give

$$w_p = \left[\frac{(a_0 + b_0) - \sqrt{(a_0 + b_0)^2 - 4\theta a_0 b_0}}{2\theta}\right]\overline{f(L)} \qquad (28)$$

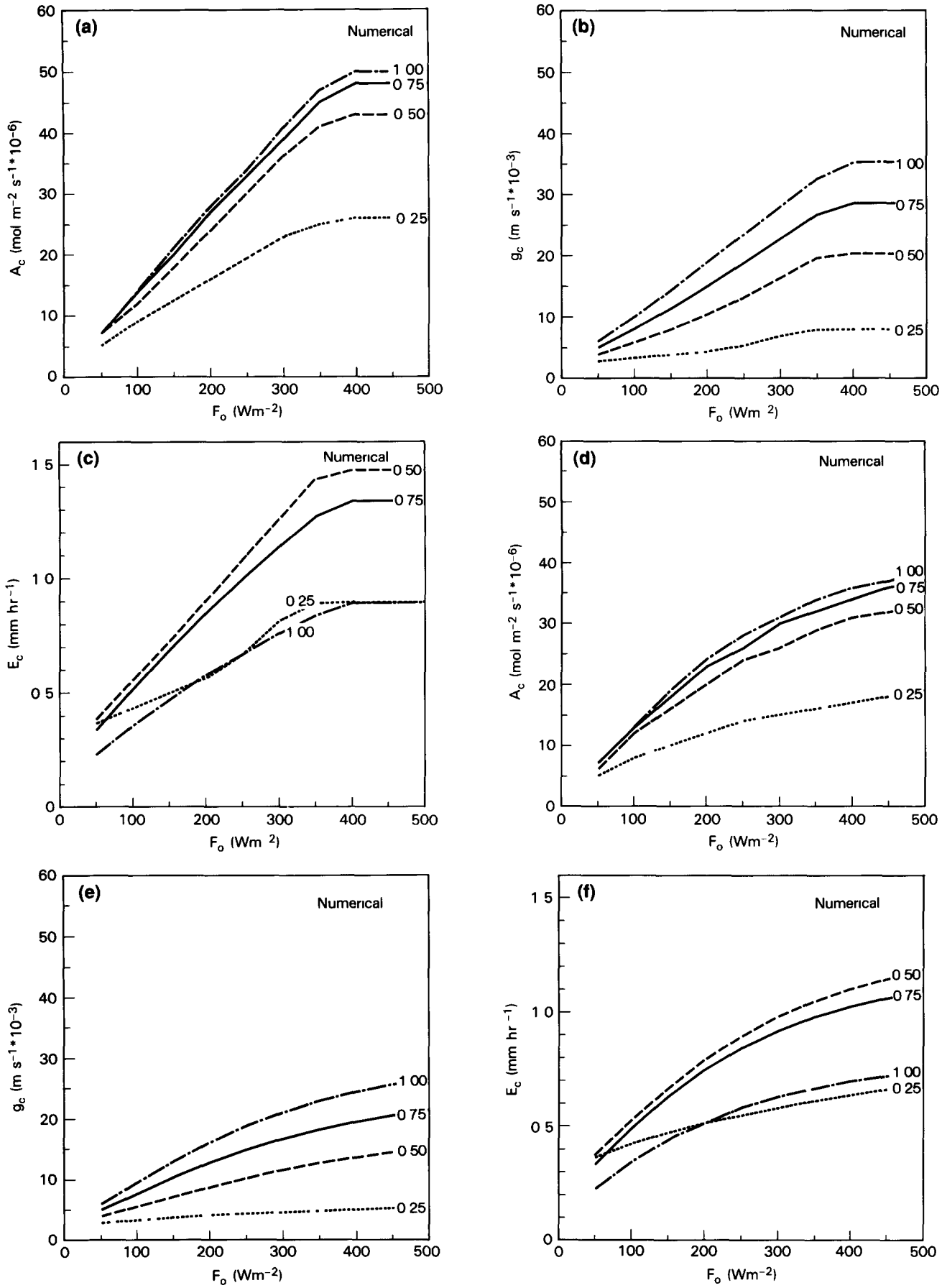

Figure 7 Canopy ($L_T = 8\ 0$) photosynthesis A_c, conductance g_c, and transpiration E_c plotted against PAR ($\mu = 0\ 5$) for different values of canopy air space relative humidity (h_a), h_a is marked on each curve *Numerical method* a) A_c, b) g_c, c) E_c for θ, $\beta = 1$, d) A_c, e) g_c, f) E_c for θ, $\beta = 0\ 8$

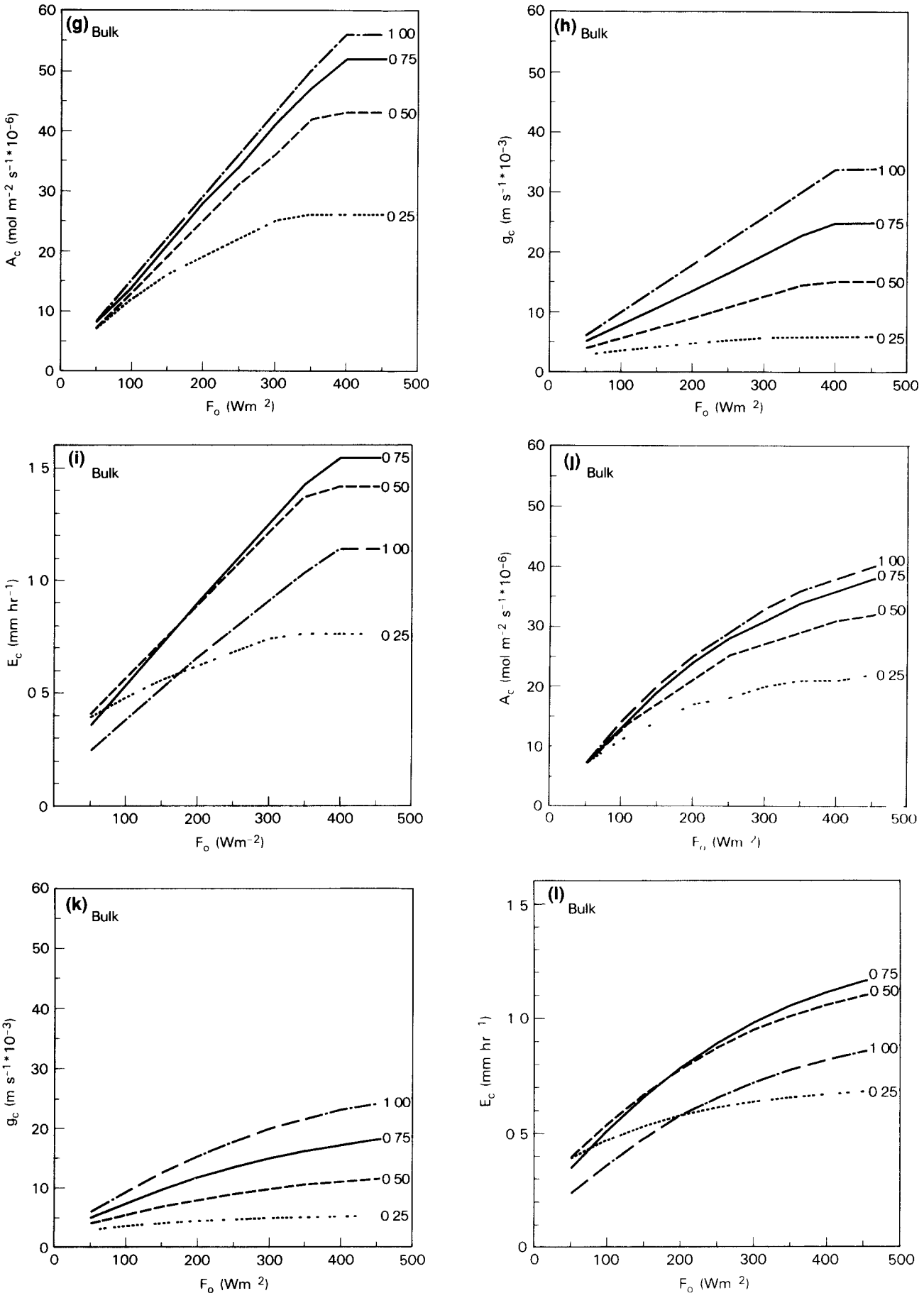

Figure 7 (continued) *Bulk method* g) A_c, h) g_c, i) E_c for θ, $\beta = 1$, j) A_c, k) g_c, l) E_c for θ, $\beta = 0\,8$

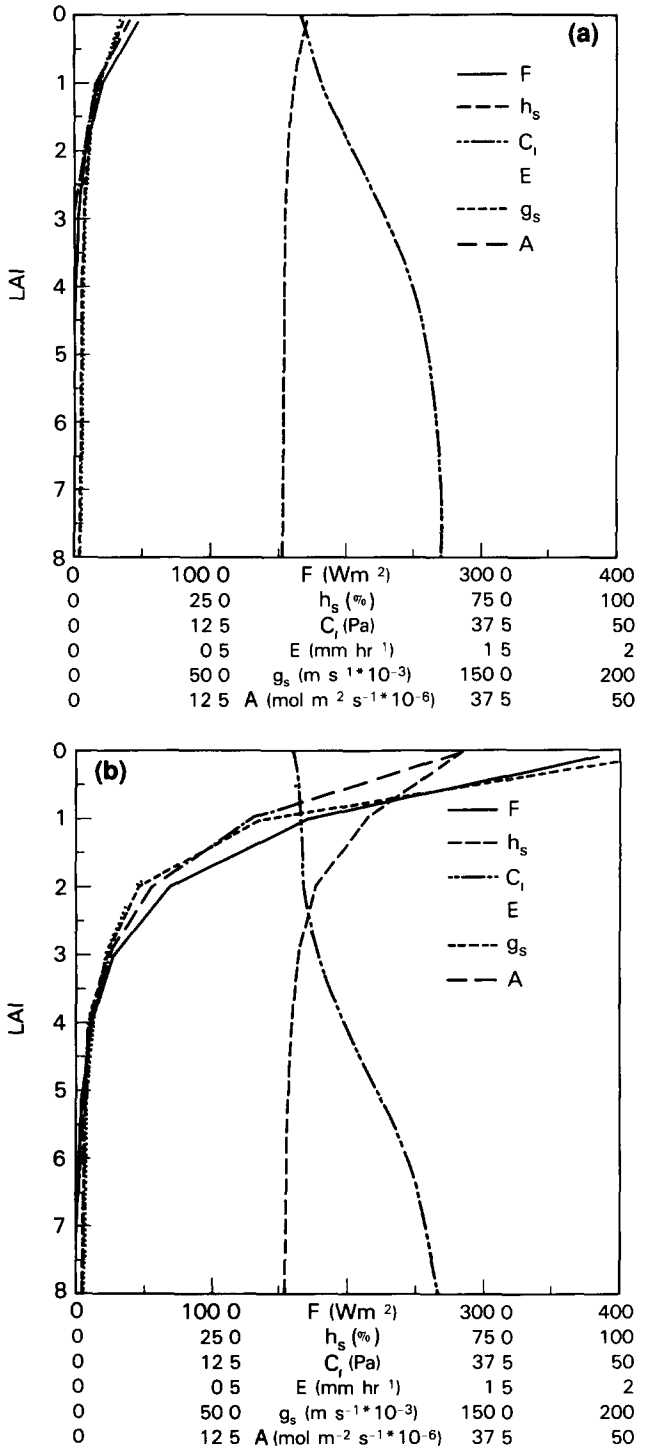

Figure 8 Profiles of PAR flux, F, leaf surface relative humidity h_s, leaf internal CO_2 concentration C_i, leaf transpiration E, leaf conductance g_s, leaf assimilation A θ, $\beta = 1\ 0$, $h_a = 0\ 5$, $\mu = 0\ 5$, $R_d = 0$ all other parameters as in Table 2 a) $F_0 = 50$ W m^{-2}, b) $F_0 = 400$ W m^{-2}

The use of the bulk values C_I, h_s, and C_s allows us to integrate (28) over the depth of the canopy to obtain w_P simply by integrating the $f(L)$ term

$$w_P = \left[\frac{(a_0 + b_0) - \sqrt{(a_0 + b_0)^2 - 4\theta a_0 b_0}}{2\theta}\right] \times \int_0^{L_T} \overline{f(L)}\ dL \tag{29}$$

In the simple case of a homogeneous canopy, we can substitute Eq (25) into (29) to yield

$$w_P = \left[\frac{(a_0 + b_0) - \sqrt{(a_0 + b_0)^2 - 4\theta a_0 b_0}}{2\theta}\right] \times \left[\frac{1 - e^{-\bar{k}L_T}}{\bar{k}}\right] \tag{30}$$

Note that the second term in parenthesis can be written as

$$\Pi = \int_0^{L_T} \overline{f(L)}\ dL = \left[\frac{1 - e^{-\bar{k}L_T}}{\bar{k}}\right] \simeq \frac{\overline{FPAR}}{\bar{k}} \tag{31}$$

In Eq (30), the first term in parenthesis is simply the photosynthetic rate of the "top" leaves in the canopy, that is, those with the highest photosynthetic capacity, V_{max0}, exposed to the highest time-mean PAR flux, $\bar{F}_0$, and subject to C_I, h_s, and C_s The second term, defined as Π in (31), acts as a simple scaling-up factor to relate the "top" leaf performance to canopy performance

The canopy equivalent of w_s, w_s, is given by rearranging Eq (12) to give

$$w_s = \int_0^{L_T} \frac{V_m\ dL}{2} = \frac{V_{m0}}{2} \int_0^{L_T} \overline{f(L)}\ dL \tag{32}$$

w_s and w_P can then be inserted into (14b) to determine A_C, the canopy gross assimilation rate

The canopy respiration rate can be given by

$$R_D = \int_0^{L_T} R_d\ dL = R_{d0} \int_0^{L_t} \overline{f(L)}\ dL \tag{33}$$

Equations (30), (32), and (33) can be combined to give the net canopy assimilation rate A_N As the integral of $\overline{f(L)}$ occurs in all three equations, A_N can be written as

$$A_N = A_{n0} \cdot \Pi, \tag{34}$$

$$A_{n0} = f(a_0, b_0, V_{m0}, R_{d0}),$$

where Π is given by Eq. (31)

A_{n0} is effectively the "single leaf" solution to Eqs (11)–(15) where constants appropriate to the

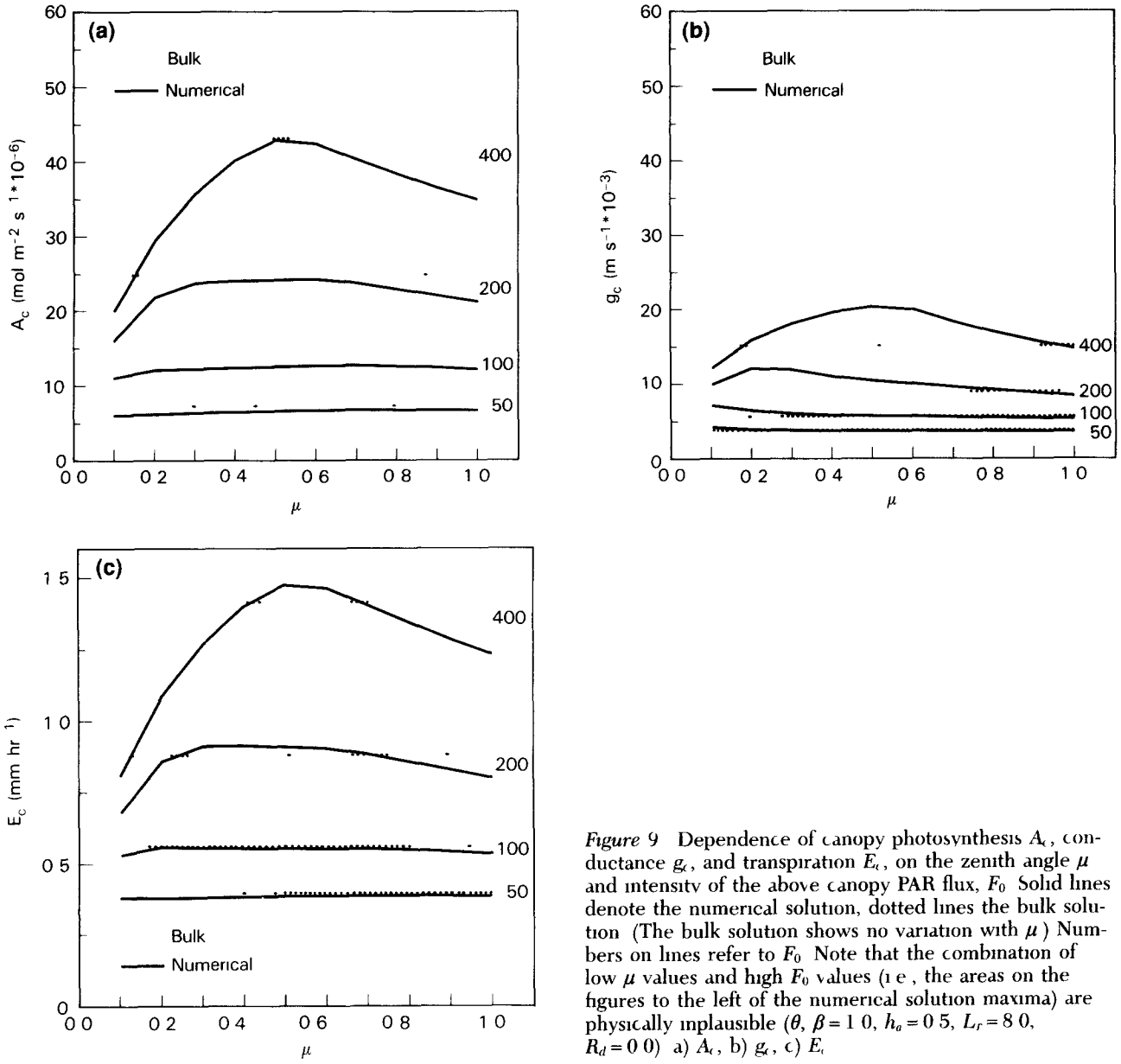

Figure 9 Dependence of canopy photosynthesis A_c, conductance g_c, and transpiration E_c, on the zenith angle μ and intensity of the above canopy PAR flux, F_0 Solid lines denote the numerical solution, dotted lines the bulk solution (The bulk solution shows no variation with μ) Numbers on lines refer to F_0 Note that the combination of low μ values and high F_0 values (i e , the areas on the figures to the left of the numerical solution maxima) are physically implausible (θ, $\beta = 1\ 0$, $h_a = 0\ 5$, $L_T = 8\ 0$, $R_d = 0\ 0$) a) A_c, b) g_c, c) E_c

"top" leaves are used, Π is the canopy-integral term which is dependent not only on $\overline{FPAR}$ but also on how the PAR is absorbed through the canopy, that is, canopy architecture, as specified by $\bar{k}$

The combined canopy model is then completed with an integral form of the conductance equation (17)

$$g_c = \frac{mA_N}{C_s} h_s p + bL_T, \qquad (35)$$

where A_N, h_s, and C_s are bulk canopy values In Eq (35), it is assumed that all leaves have the same "leakage" conductance b when $A_N = 0$

The system of equations corresponding to Figure 5c now consists of (27), (29), (31), (32), and (33) [summarized in (34)] and (35) These can be solved in exactly the same way as for a single leaf (see Fig 4)

The assumptions and simplifications involved in going from the system shown in Figure 5b to that in Figure 5c are nontrivial, μ is set equal to $\bar{\mu}$ and the variables C_i, h_s, C_s, g_s, and g_b are all replaced by bulk canopy values It is therefore

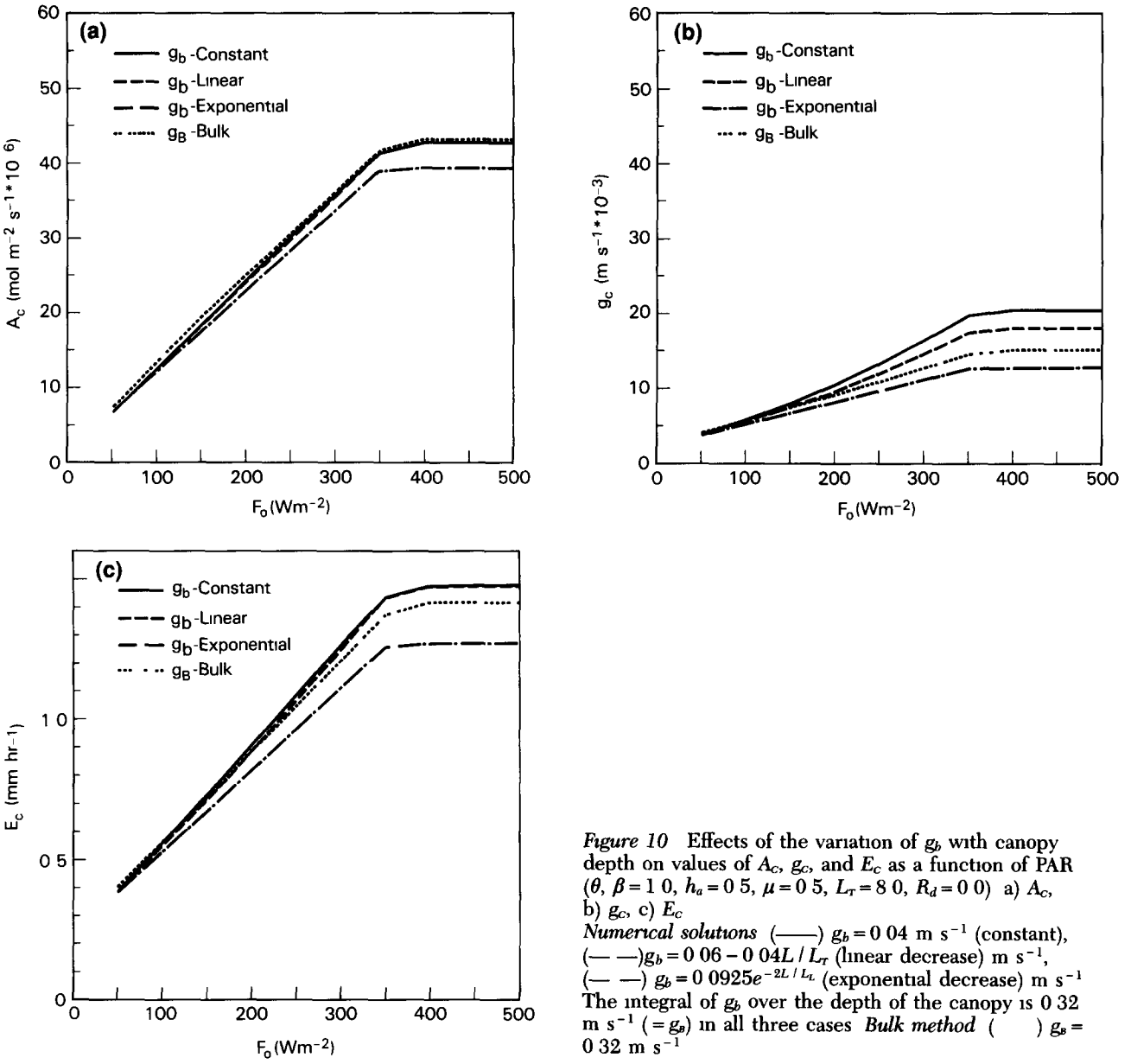

Figure 10 Effects of the variation of g_b with canopy depth on values of A_c, g_c, and E_c as a function of PAR (θ, $\beta = 1\ 0$, $h_a = 0\ 5$, $\mu = 0\ 5$, $L_T = 8\ 0$, $R_d = 0\ 0$) a) A_c, b) g_c, c) E_c
Numerical solutions (——) $g_b = 0\ 04$ m s^{-1} (constant), (— —)$g_b = 0\ 06 - 0\ 04L / L_T$ (linear decrease) m s^{-1}, (— —) $g_b = 0\ 0925e^{-2L/L_L}$ (exponential decrease) m s^{-1} The integral of g_b over the depth of the canopy is 0 32 m s^{-1} ($= g_B$) in all three cases *Bulk method* ( ) $g_B = 0\ 32$ m s^{-1}

interesting to explore the differences between the solutions given by the two methods

Figures 7g–l show the bulk method estimates of A_c, g_c and E_c for the optimal case $\bar{\mu} = \mu$, the solutions are always within a few percent of the numerical scheme solutions, see Figures 7a–f

Figures 9 and 10 compare the values of A_c, g_c, and E_c as given by the two methods over a range of PAR vectors and for a range of g_b profiles Except for the extreme and physically implausible case of low values of μ combined with high values of F_0, the bulk method yields fluxes that are close to those of the numerical scheme

Figure 11 compares the values of g_c h_s, and C_i as given by the two integration schemes Weighted estimates of g_c, h_s, and C_i for the numerical scheme are given by

$$g_c = \frac{1}{L_T}\int_0^{L_T} g_s \, dL, \tag{36a}$$

$$h_s = \frac{1}{L_T}\int_0^{L_T} h_s \, dL, \tag{36b}$$

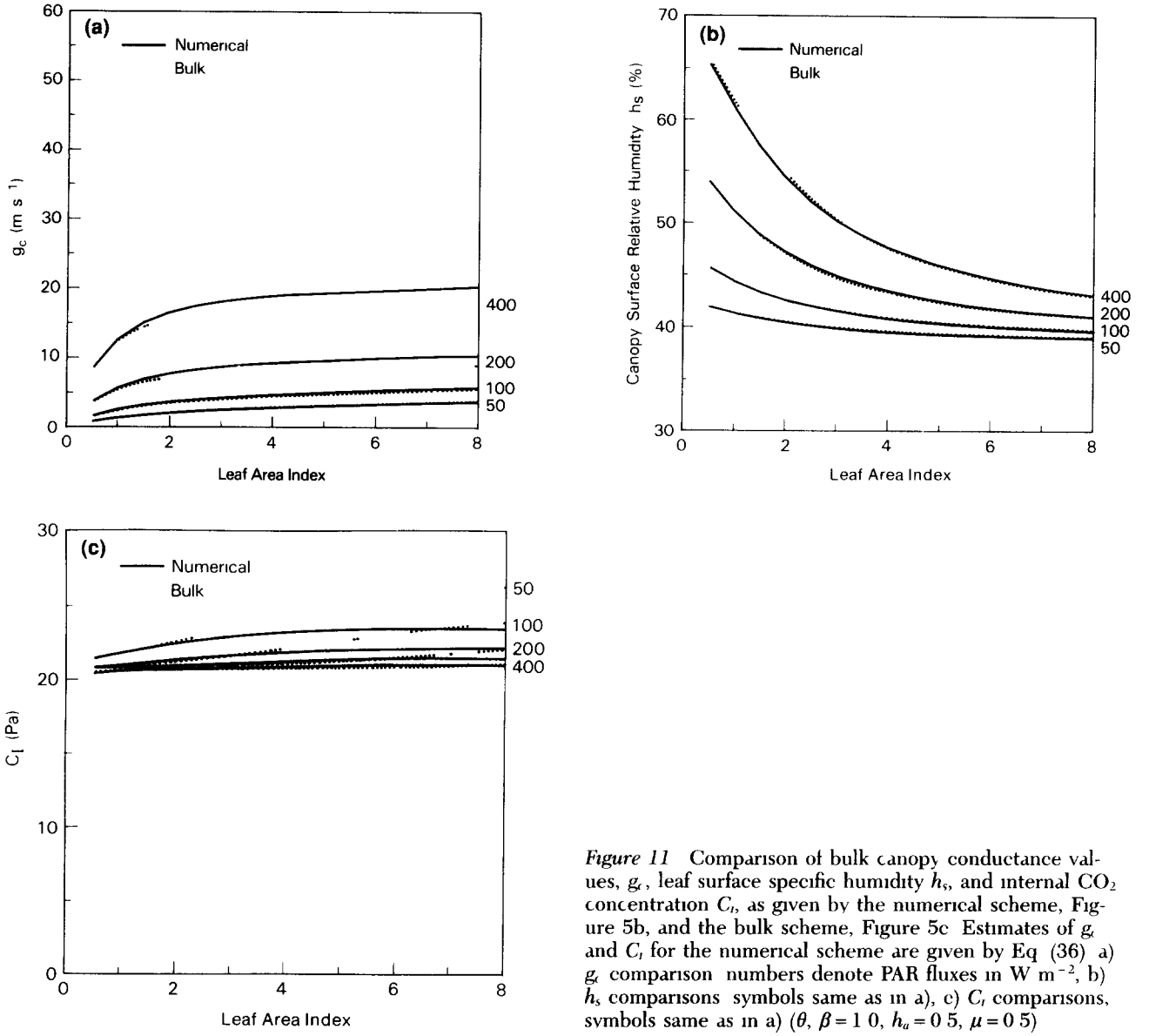

Figure 11 Comparison of bulk canopy conductance values, g_c, leaf surface specific humidity h_s, and internal CO_2 concentration C_i, as given by the numerical scheme, Figure 5b, and the bulk scheme, Figure 5c Estimates of g_c and C_i for the numerical scheme are given by Eq (36) a) g_c comparison numbers denote PAR fluxes in W m^{-2}, b) h_s comparisons symbols same as in a), c) C_i comparisons, symbols same as in a) (θ, $\beta = 1\ 0$, $h_a = 0\ 5$, $\mu = 0\ 5$)

$$C_i = \frac{1}{A_c L_T} \int_0^{L_T} AC_i \, dL \qquad (36c)$$

The bulk model yields integrated estimates of these state variables that are close to those calculated with the numerical scheme

RELATING CANOPY BIOPHYSICAL PROPERTIES TO SPECTRAL REFLECTANCES

Equations (34) and (35) appear to be effective canopy-integral forms of the leaf or chloroplast level formulations of Farquhar et al (1980) and Collatz et al (1991) The nonlinear effects induced by varying solar angles and the profile gradients of governing state variables (C_i, h_s, g_b, etc) within the canopy do not prevent the bulk integral method from providing useful estimates of the fluxes of CO_2 and H_2O under normal conditions

The inclusion of these more sophisticated physiological models into the analysis leads to different canopy biophysical–spectral reflectance relationships than those described by Sellers (1987)

We can rewrite the canopy-integral equations

for the rate limiting processes governing photosynthesis as follows

$$w_C = v_{m0}\,\Pi B_1, \tag{37a}$$

$$w_E = F_0\,\Pi B_2, \tag{37b}$$

$$w_S = V_{m0}\,\Pi B_3, \tag{37c}$$

$$R_D = V_{m0}\,\Pi B_4, \tag{37d}$$

$$A_C = A_{n0}\,\Pi B_5 = f(w_C, w_E, w_S) - R_D, \tag{37e}$$

$$g_C \approx A_{n0}\,\Pi B_6, \tag{37f}$$

where

$$B_1 = \left[\frac{C_I - \Gamma^*}{C_I + K_c[1 + O_2/K_o]}\right],$$

$$B_2 = \frac{G(\bar{\mu})}{\bar{\mu}}(1 - \omega_v)\varepsilon\left[\frac{C_I - \Gamma^*}{C_I + 2\Gamma^*}\right],$$

$$B_3 = 0\,5,$$

$$B_4 = 0\,015,$$

$$B_5 = 1\,0,$$

$$B_6 = \frac{mh_s p}{C_s}$$

In Eq (37), the canopy biophysical variables (left-hand side) are calculated as the product of three parameters or forcing variables (right-hand side) These parameters / forcing variables can be described as follows

First Variable: Plant Physiology or Radiation Rate Limit Variable (V_{m0}, $\mathbf{F}_0$, A_{n0})

V_{m0} or F_0 are the rate limiting factors governing the canopy response at saturating PAR fluxes and less than saturating PAR fluxes respectively A_{n0}, appearing in (37e) and (37f), is a direct function of these two variables Previous sections have discussed the functional dependence of V_{m0} on $\overline{\mathbf{F}_0\ \mathbf{n}}$ The time history of $\overline{\mathbf{F}_0 \cdot \mathbf{n}}$ can be obtained from satellite climatological studies, for example, Frouin and Gautier (1990) demonstrated how Geostationary Operational Environmental Satellite (GOES) data could be used to compute the diurnally varying PAR flux over a Kansas grassland area (the FIFE site) with a surface resolution of around 1 km^2 Such data could be composited to provide a global PAR climatology from which seasonally-varying, time-mean fields of $\mathbf{F}_0 \cdot \mathbf{n}$ could be produced The dependence of A_C and g_C on F_0 is obvious

$$\frac{\partial A_C}{\partial F_0}, \frac{\partial g_C}{\partial F_0} = \Pi B_5, \Pi B_6, \quad \text{for } F_0 < V_{m0}\frac{B_1}{B_2} \tag{38a}$$

$$= 0, \quad \text{for } F_0 > V_{m0}\frac{B_1}{B_2} \tag{38b}$$

Equation (38) indicates that for nonsaturating PAR fluxes, the unstressed canopy photosynthetic rate and conductance respond almost linearly with changes in PAR with a slope that is directly proportional to Π and FPAR The effects of environmental stress or forcing are contained within the B_5 and B_6 terms Equation (38) holds for θ, $\beta \to 1$, lower values of θ and β will give a gradual transition from (38a) to (38b) with increasing F_0

Equation (38) and the supporting analysis indicate that all the leaves in the canopy saturate at the same value of $F_0 = V_{m0}(B_1 / B_2)$ This is because V_m is scaled according to the time-mean profile of PAR within the canopy

Second Variable: Canopy PAR Use Parameter (II)

This parameter corresponds to $\overline{\text{FPAR}}$ divided by the PAR extinction parameter $\bar{k}$ It is the scaling parameter that relates canopy performance to the performance of the "top" leaves Typically, $\bar{k}$ varies between 0 4 and 1, so that a continuous fully developed canopy ($\overline{\text{FPAR}} \simeq 1$) will perform at between one and three times the rate defined by the ensemble of "top" leaves

FPAR is the vegetation parameter most readily amenable to remote sensing [see Asrar et al (1984), Tucker et al (1981), Sellers (1985, 1987), Hall et al (1990), and papers in Asrar (1990)]. From this analysis, it appears that the value of FPAR associated with the radiation-weighted time-mean PAR flux vector $\overline{\mathbf{F}_0}$ [see Eq (25)] combined with the corresponding value of $\bar{k}$, is the most useful canopy parameter for biophysical calculations This implies that multiangle data should be acquired over vegetation canopies at solar angles corresponding to $\bar{\mu}$ to obtain estimates of $\overline{\text{FPAR}}$ and $\bar{k}$

If we neglect second-order feedback effects (see next section), all of the canopy biophysical rates are linear in Π [see Eqs (37) and (38)]

This represents a distinct improvement over the analysis of Sellers (1985) as now the contribution of canopy density and morphology (Π) is cleanly separated from those of leaf physiology and radiation flux (V_{m0}, F_0) Sellers (1987) showed how under ideal conditions the simple ratio vegetation index, SR, was linearly related to FPAR provided that Eq (3) holds for the vegetation / type viewing sensor combination and the soil background is fairly dark The chain of relationships

$$g_c, A_c \propto \Pi \propto \text{FPAR} \propto \text{SR} \qquad (39a)$$

or, simply,

$$A_c = f_A(\text{SR}), \qquad (39b)$$

$$g_c = f_g(\text{SR}), \qquad (39c)$$

where f_g and f_A are near-linear functions when $\mu \rightarrow \bar{\mu}$, indicates that SR or other SVI images may be used to calculate fields of A_c, g_c, and E_c using a simple linear transform of the image combined with environmental forcings (F_0, H_a, T_a, C_a, soil moisture stress, etc) and some knowledge of the leaf physiology (V_{m0}, m, etc) In grasslands or areas with drought-deciduous vegetation, it is reasonable to assume that chronic soil moisture stress will be expressed as a decrease in Π so that direct

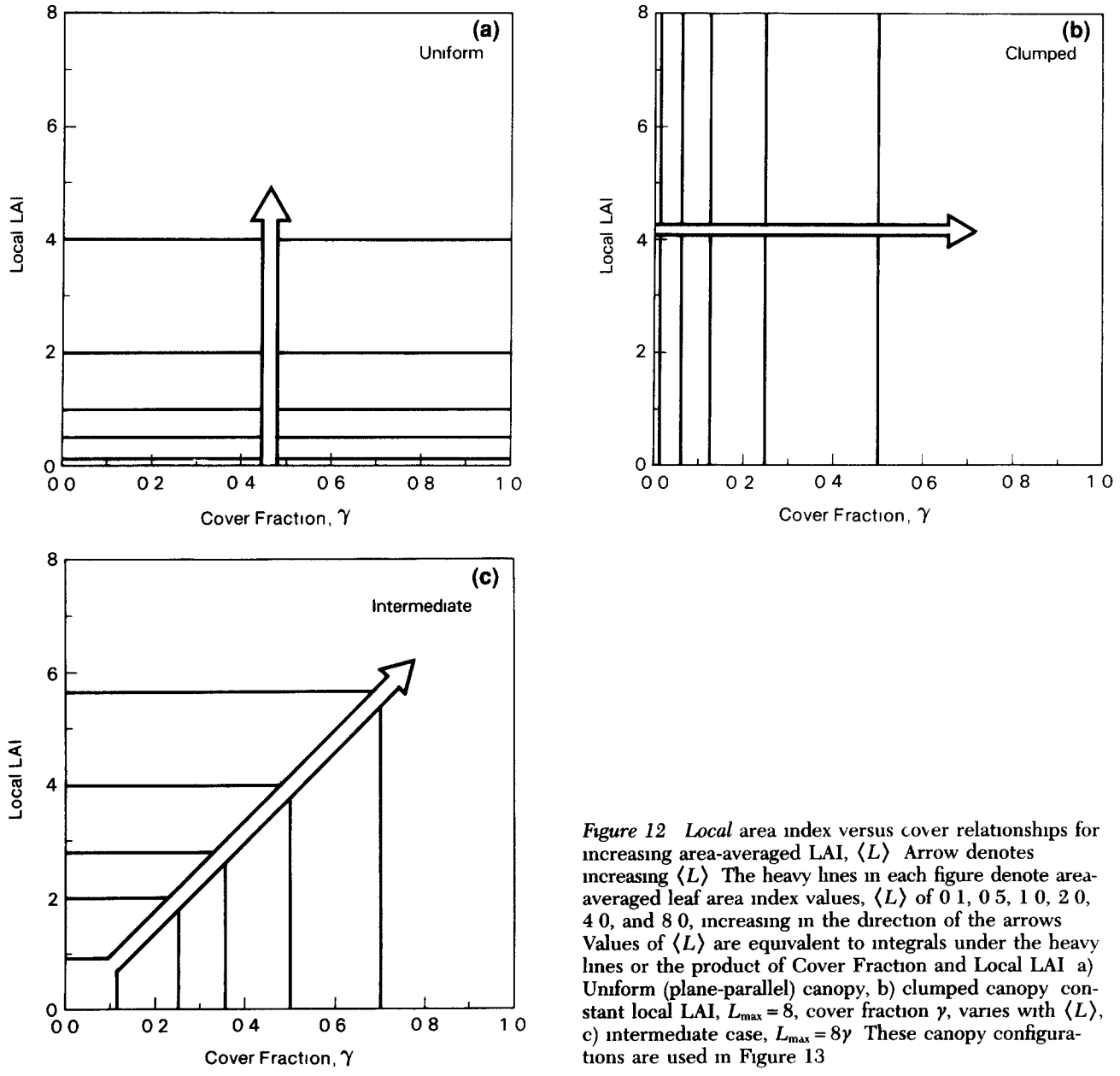

Figure 12 *Local* area index versus cover relationships for increasing area-averaged LAI, $\langle L \rangle$ Arrow denotes increasing $\langle L \rangle$ The heavy lines in each figure denote area-averaged leaf area index values, $\langle L \rangle$ of 0 1, 0 5, 1 0, 2 0, 4 0, and 8 0, increasing in the direction of the arrows Values of $\langle L \rangle$ are equivalent to integrals under the heavy lines or the product of Cover Fraction and Local LAI a) Uniform (plane-parallel) canopy, b) clumped canopy constant local LAI, $L_{max} = 8$, cover fraction γ, varies with $\langle L \rangle$, c) intermediate case, $L_{max} = 8\gamma$ These canopy configurations are used in Figure 13

knowledge of the soil moisture content might not be essential

In nature, variations in area-averaged leaf area index can occur in two ways First, a horizontally uniform canopy may vary in thickness (vertical dimension) This was the case studied by Sellers (1987), which led to the result that FPAR would be linearly related to SR (see Fig 12a) A second way is for the canopy to vary in area-averaged cover fraction This is often the case for coniferous trees or desert shrubs where the leaf area of an individual tree remains relatively constant, but plant abundance varies depending on ecological conditions (see Fig 12b) Hall et al (1990) used this second scenario to explore the utility of spectral second derivatives and SR data to determine FPAR, once again, these indices were more or less linear with FPAR A simple analysis is presented below which demonstrates that while the relationship between area-averaged leaf area index and FPAR (and therefore spectral vegetation indices, SVI) will vary depending on the horizontal and vertical distribution of the vegetation, the relationship between FPAR, SVI and A_c, g_c remains invariant

Up to now, we have considered a plane parallel canopy of leaf area index L_T Let us now consider a landscape made up of identical homogeneous vegetation units, rather like box hedges, each with a *local* leaf area index of L_{max} and covering a total fraction γ of the landscape (or instrument field of view) Thus,

$$\langle \text{FPAR} \rangle = \gamma(1 - e^{-\bar{k}L_{max}}) \qquad (40a)$$

The area-averaged leaf area index is given by

$$\langle L_T \rangle = \gamma L_{max}, \qquad (40b)$$

where the $\langle\ \rangle$ symbols denote "area average"

Figure 13 shows the relationship between FPAR and $\langle L_T \rangle$ for different degrees of "clumping" (values of γ) Clearly, as γ decreases, $\langle L_T \rangle$ must increase to maintain the same value of FPAR

However, an inspection of Eq (37) and the supporting analysis shows that A_c and g_c are dependent on Π, that is, on $\overline{\text{FPAR}}/\bar{k}$, and not on the spatial distribution of the vegetation density, provided that one ignores variations in the forcing/feedback terms B_1–B_6 If we look at a vegetated region of area S, containing clumps of vegetation of varying size and density, but all having the same

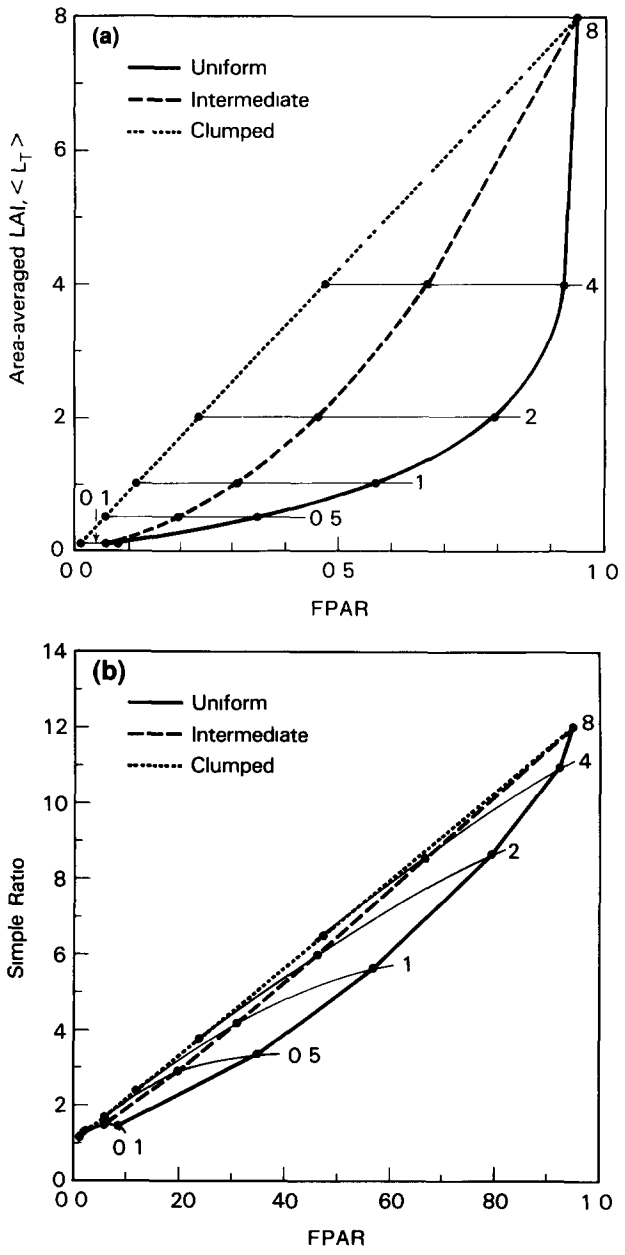

Figure 13 Variation of a) area-averaged total leaf area index $\langle L_T \rangle$ with FPAR, and b) simple ratio vegetation index with FPAR for different levels of "clumpiness" parameters from Table 1 In a) and b), the thin lines ending in numbers refer to values of area-averaged leaf area index, $\langle L_T \rangle$ (——) Spatially uniform canopy, $\gamma = 1$ L_T varies from 0 to 8, ( ) clumped canopy, $\gamma = 0$ to 1, $L_{max} = 8$, (- - -) intermediate case, $L_{max} = 8\gamma$ Refer also to Fig 12

baseline physiology (V_{max0}) and leaf geometric/spectral properties ($\bar{k}$, ω_v) overlying a soil background of uniform reflectance, we can write

$$\langle A_c, g_c \rangle = \frac{1}{S}\int_0^S A_c, g_c \, ds \qquad (41a)$$

$$\propto \frac{1}{S}\int_0^s \Pi_i \, \mathrm{SVI} \; ds, \qquad (41b)$$

where SVI, the spectral vegetation index, is SR or a spectral second derivative index (see Hall et al , 1990)

Now for a linear function, the area-integral and spatial average (multipled by the area) operators are equivalent

$$\langle \; \rangle \equiv \frac{1}{S}\int_0^s ds \qquad (42)$$

Since the functions relating A_c, g_c and Π_i SVI are linear or nearly so, we can rewrite (41) as

$$\langle A_c, g_c \rangle = \frac{1}{S}\int_0^s A_c, g_c \; ds \propto \langle \Pi \rangle \propto \langle \mathrm{SVI} \rangle \qquad (43)$$

Equation (43) represents a powerful and

Figure 14 Variation of canopy photosynthesis A_c and conductance g_c with FPAR as calculated using the coupled stomatal–photosynthesis model (bulk scheme) shown in Figure 5c Different spatial distributions of $\langle L \rangle$ are used corresponding to those shown in Figure 12 Dots denote values of $\langle L \rangle = 0\,1,\ 0\,5,\ 1\,0,\ 2\,0,\ 4\,0,\ 8\,0$ (——) Spatially uniform canopy, $\gamma = 1$, L_T varies from 0 to 8 ( ) clumped canopy, $\gamma = 0$ to 1, $L_{max} = 8$, (– – –) Intermediate case, $L_{max} = 8\gamma$ a b) A_c and g_c, $h_a = 1$, c,d) A_c and g_c, $h_a = 0\,5$ (θ, $\beta = 0\,8$, $F_0 = 400$ W m^{-2}, $\mu = 0\,5$)

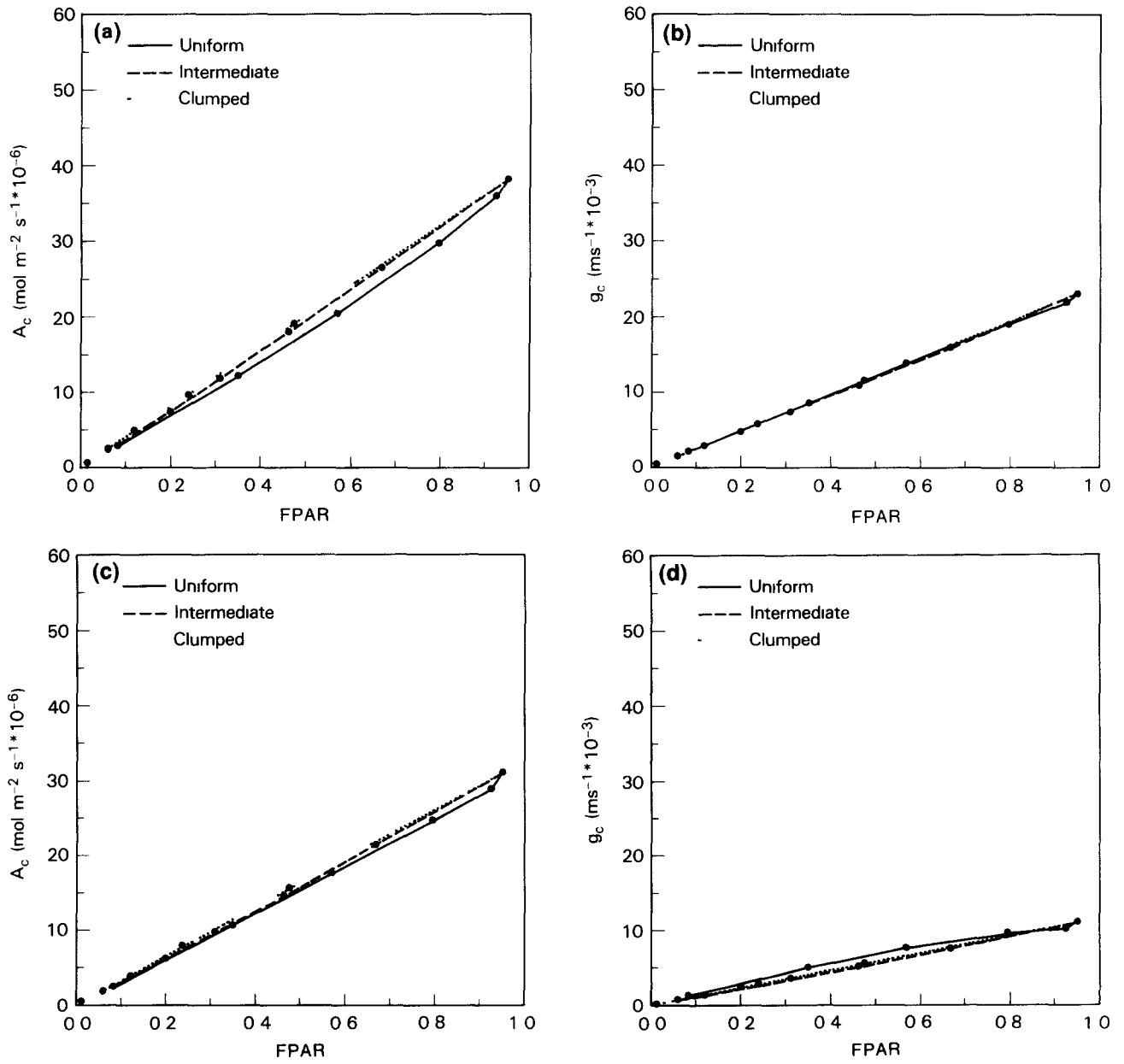

counterintuitive result· The *mean* value of SVI as measured over an area should vary linearly with the areal integral and/or mean values of Π, A_C, and g_C, to first order In areas with very high local values of L_T, higher-order effects (feedbacks between the vegetation and its immediate environmental through C_s, h_s, etc) may act to vary the coefficients B_1–B_6 and cause some local distortion of this relationship However, it is interesting that the inclusion of the ecophysiological optimality assumption of Eq (21) into the equation set maintains the linearity of the SVI versus Π, A_C, g_C relationship over a wide range of spatial scales and over heterogeneous vegetation density distributions (see Fig 14) This is a very different result from that obtained by Sellers (1985), who assumed invariant leaf physiology within the canopy, that is, $V_{max} = V_{max0}$ for all L, and therefore derived a range of SVI versus A_C, g_C relationships depending on the value of γ (see Fig 15)

Third Variable: Environmental Forcing or Feedback Term (B_i)

For a given set of environmental conditions, the variables B_3, B_4, and B_5 can be effectively considered as constants over the area of integration, S The variables B_1, B_2, and B_6 are the result of interactions between the vegetation biophysical process rates and the environmental forcings, the linkages being through C_I, h_s, and C_s These feedbacks are functionally the same as those for a single leaf (see Collatz et al , 1991)

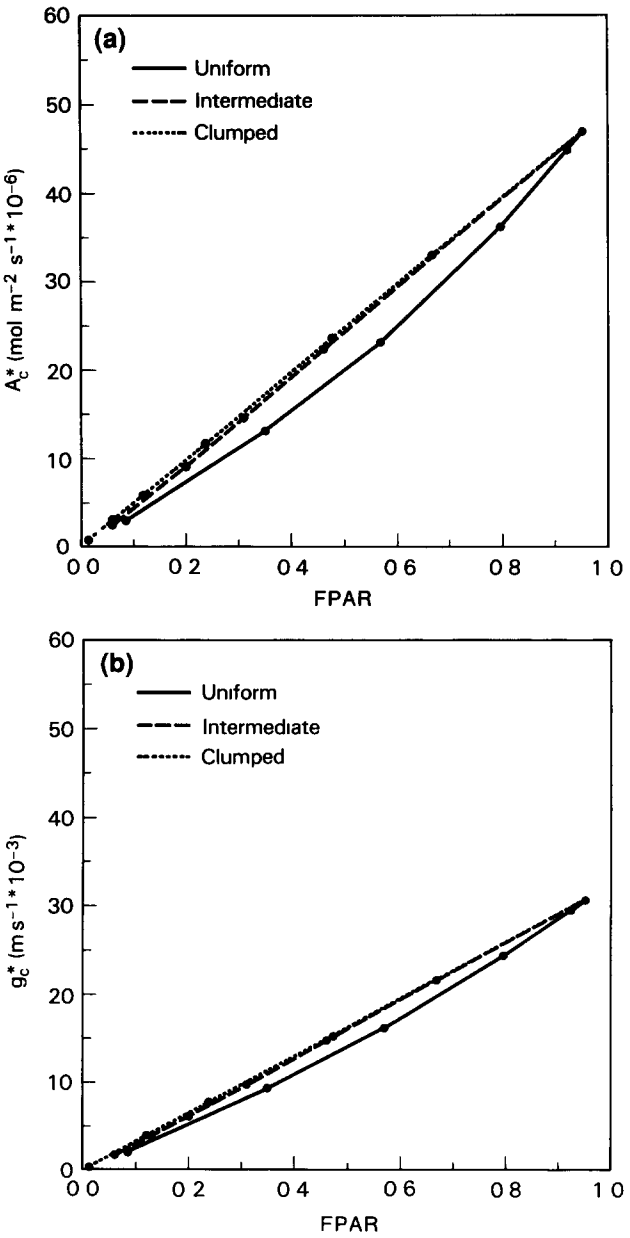

Figure 15 Variation of canopy photosynthesis A_C and conductance g_C with FPAR, as calculated with empirical leaf models in Eq (5), following methods described in Sellers (1985) All symbols and conditions are the same as in Figures 14a and 14b a,b) A_C and g_C, $f(\Sigma) = 1$ (Canopy, soil properties from Table 1, $F_0 = 400$ W m^{-2}, $\mu = 0\,5$) Note that these values of A_C and g_C are higher than those shown in Figures 14a and 14b This is because *all* the leaves in the canopy have the same biophysical properties as the "top leaf", see Figures 1, 6c, and 6g Additionally, A_C and g_C are shown to vary markedly with vegetation heterogeneity using the methods of Sellers (1985) whereas, in the new formulation, they do not, compare with Figures 14a and 14b

SUMMARY

The leaf photosynthetic model of Farquhar et al (1980) and the leaf conductance model of Collatz et al (1991) can be analytically integrated over the depth of a vegetation canopy provided some simplifying assumptions are made In practice, the bulk analytical canopy model yields values of net canopy assimilation rate A_C, canopy conductance g_C, and canopy transpiration E_C that are close to those provided by an exact (numerical) integration of the leaf models for normal environmental conditions

In defining the properties of the model canopy, the arguments of ecophysiological optimality, as invoked by Farquhar (1989) to describe the profile of chloroplast Rubisco content within a leaf, were used to define the profile of leaf Rubisco content, V_{max}, within the canopy so that the re-

sulting profile of V_{max} follows the time-mean profile of PAR through the canopy

As a result, the contributions of leaf physiology, canopy density and geometry, and environmental forcing are separable in the integrated bulk canopy model, this was not the case for the "simpler" models used by Sellers (1985, 1987) This finding, Eq (37), may be summarized by

$$\begin{array}{lcccc} \text{Canopy biophysical rate variable} & = & \left[\begin{array}{c}\text{Leaf physiology or radiation rate limit}\end{array}\right] & \left[\begin{array}{c}\text{Canopy PAR use parameter}\end{array}\right] & \left[\begin{array}{c}\text{Environmental forcing or feedback}\end{array}\right] \\ A_C, g_C = & & [V_{max0}, F_0] & [\Pi] & [B_1, \quad B_6] \end{array} \tag{37}$$

This revised canopy model has the following interesting and useful properties

i. **Near-linear relationship between A_C, g_C and incident PAR flux, F_0, for values of F_0 less than saturation. All leaves within the canopy saturate at the same value of F_0 due to the variation of V_{max} with depth.**

ii. **Linear relationship between A_C, g_C and the canopy PAR use parameter Π, where Π is equal to the radiation-weighted time-mean of canopy FPAR divided by the extinction coefficient for PAR, $\bar{k}$**

It should be possible to estimate Π by taking multiangle reflectance data over a target area for solar angles that correspond to the optimal time-mean PAR flux ($\mu = \bar{\mu}$) as defined by Eq (26)

iii. **Linear relationships between A_C, g_C, Π, and SVI simplify area-averaged biophysical calculations.**

The SVI can be configured to yield a linear relationship with FPAR and hence Π [see Eq (2)] This is true whether one considers a canopy varying in depth (Sellers, 1985, 1987) or areal cover fraction (Hall et al , 1990) or a heterogeneous combination of both Given such a condition (SVI$\propto$FPAR, Π) and an area containing vegetation of uniform physiology, leaf geometry, and spectral properties overlying a uniform background, the mean SVI for an area can be used to directly calculate the area integrals of the canopy photosynthetic rate A_c and conductance g_C

$$\frac{1}{S}\int_o^s A_c, g_C \; ds = f_A(\langle \mathrm{SVI} \rangle), F_g(\langle \mathrm{SVI} \rangle), \tag{44}$$

where the functions f_A, f_g are the same (near-linear) functions relating canopy assimilation and conductance, respectively, to the SVI as those derived for a small-scale homogeneous vegetation cover (i e , a sample in the area) The angle brackets denote "area average "

The simplicity of these relationships should permit straightforward transformation of satellite imagery—time series of F_0 from GOES data superposed on fields of SVI—to calculate regional fields of the (soil-moisture stress-free) canopy photosynthetic rates A_c, conductances g_c, and transpiration rates E_C The linearity of the SVI–II relationship should permit the use of coarse spatial resolution satellite imagery for this application

Funding support for this work was supplied by an Earth Observing System / Interdisciplinary Science (EOS-IDS) grant from NASA and a NASA grant for FIFE-related studies (NAG-5-892) The support of many people at NASA HQ and NASA / GSFC is gratefully acknowledged At Carnegie Institution, Cyril Grivet provided technical assistance David Schimel and Fred Huemmrich are thanked for interesting discussions Much of the analysis was conducted at the University of Maryland under the aegis of the Center for Ocean–Land–Atmosphere Interactions (COLA) and the Department of Meteorology The support of these institutions and the help of Mark Heiser, who prepared the graphs, and Marlene Schlichtig, who typed the paper, is gratefully acknowledged

REFERENCES

Asrar, G , (Ed) (1990), *Theory and Applications of Optical Remote Sensing*, Wiley-Interscience, New York, pp 734

Asrar, G , Fuchs, M , Kanemasu, E T, and Hatfield, J L (1984), Estimating absorbed photosynthetic radiation and leaf area index from spectral reflectance in wheat, *Agron J* 76 300–306

Ball, J T (1988), An analysis of stomatal conductance, Ph D thesis Stanford University, 89 pp

Bazzaz, F A , (1979), The physiological ecology of plant succession, *Annu Rev Ecol Syst* 10 351–371

Bjorkman, O (1981), Responses to different quantum flux densities, in *Encyclopedia of Plant Physiology, Vol 12A Plant Physiological Ecology I* (O L Lange, P S Nobel, C B Osmond and H Ziegler, Eds), Springer-Verlag, Berlin, pp 57–107

Bjorkman, O , and Holmgren, P (1963), Adaptability of the photosynthetic apparatus to light intensity in ecotypes from exposed and shaded habitats, *Physiol Planta* 16 889–914

Bloom, A J , Chapin, F S , III, and Mooney, H A (1985), Resource limitation in plants—an economic analogy, *Annu Rev Ecol System* 16 363–392

Chapin, F S, III, Bloom, A J, Field, C B, and Waring, R H (1987), Plant responses to multiple environmental factors, *BioScience* 38 49–57

Charles-Edwards, D A, and Ludwig, L J (1974), A model for leaf photosynthesis by C_3 plant species, *Ann Bot* 38 921

Collatz, G J, Berry, J A, Farquhar, G D, and Pierce, J (1990), The relationship between the rubisco reaction mechanism and models of leaf photosynthesis, *Plant Cell Environ* 13 219–225

Collatz, G J, Ball, J T, Grivet, C, and Berry, J A (1991), Physiological and environmental regulation of stomatal conductance, photosynthesis and transpiration a model that includes a laminar boundary layer, *Agric For Meteorol* 54 107–136

Cowan, I R, and Farquhar, G D (1977), Stomatal function in relation to leaf metabolism and environment, *Symp Soc Exp Biol* 31 471–505

DeJong, T M, and Doyle, J F (1985), Seasonal relationships between leaf nitrogen content (photosynthetic capacity) and leaf canopy light exposure in peach (*Prunus persipicata*), *Plant Cell Environ* 8 701–706

Elheringer, J, and Bjorkman, O (1977), Quantum yields for CO_2 uptake in C_3 and C_4 plants, *Plant Physiol* 59 86–90

Evans, J R (1989a), Partitioning of nitrogen between and within leaves grown under different irradiances, *Aust J Plant Physiol* 16 533–548

Evans, J R (1989b), Photosynthesis and nitrogen relationships in leaves of C_3 plants, *Oecologia (Berlin)* 78 9–19

Farquhar, G D (1989), Models of integrated photosynthesis of cells and leaves, *Phil Trans Roy Soc Lond, Ser B, Biol Sci* 323 357–367

Farquhar, G D, von Caemmerer, S, and Berry, J A (1980), A biochemical model of photosynthetic CO_2 fixation in leaves of C_3 species, *Planta* 149 78–90

Field, C (1983), Allocating leaf nitrogen for the maximization of carbon gain leaf age as a control on the allocation program, *Oecologia* 56 341–347

Field, C (1988), On the role of photosynthetic responses in constraining the habitat distribution of rainforest plants, *Aust J Plant Physiol* 15 343–358

Field, C B, and Mooney, H A (1986), The photosynthesis-nitrogen relationship in wild plants, in *On the Economy of Plant Form and Function* (T J Givnish, Ed), Cambridge University Press, Cambridge, pp 25–55

Frouin, R, and Gautier, C (1990), Variability of photosynthetically available and total solar irradiance at the surface during FIFE a satellite description, in *Proceedings of the AMS FIFE Symposium*, AMS, Boston, pp 98–104

Goudriaan, J (1977), *Crop Micrometeorology A Simulation Study* Wageningen Center for Agricultural Publishing and Documentation, Wageningen, The Netherlands, 249 pp

Gutschick, V P, and Wiegel, F W (1988), Optimizing the canopy photosynthetic rate by patterns of investment in specific leaf mass, *Am Naturalist* 132 67–86

Hall, F G, Huemmrich, K F, and Goward, S N (1990), Use of narrow-band spectra to estimate the fraction of absorbed photosynthetically active radiation, *Remote Sens Environ* 32(1) 47–54

Hirose, T, and Werger, M J A (1987), Maximizing daily canopy photosynthesis with respect to the leaf nitrogen allocation pattern in the canopy, *Oecologia (Berlin)* 72 520–526

Hirose, T, Werger, M J A, and van Rheenen, J W A (1989), Canopy development and leaf nitrogen distribution in a stand of Carex acutiformis, *Ecology* 70 1610–1618

Intriligator, M D (1971), *Mathematical Optimization and Economic Theory*, Prentice-Hall, Englewood Cliffs, NJ

Jarvis, P G (1976), The interpretation of the variations in leaf water potential and stomatal conductance found in canopies in the field, *Phil Trans Roy Soc London, Ser B* 273 593–610

Kittel, T G F, Knapp, A K, Seastedt, T, and Schimel, D S (1990), A landscape view of biomass, LAI and photosynthetic capacity for FIFE, in *Proceedings of the AMS FIFE Symposium*, AMS, Boston, pp 66–69

Leverenz, J W, and Jarvis, P G (1980), Acclimation to quantum flux density within and between trees, *J Appl Ecol* 17 697–708

Mooney, H A (1972), The carbon balance of plants, *Ann Rev Ecol Syst* 3 315–346

Pons, T L, Schieving, F, Hirose, T, and Werger, M J A (1990), Optimization of leaf nitrogen allocation for canopy photosynthesis in Lysmachia vulgaris, in *Causes and Consequences of Variation in Growth Rate and Productivity of Higher Plants* (H Labers, M L Canbridge, H Honings, and T L Pons, Eds), SBP Academic Publishing bv, The Hague, pp 175–186

Sato, N, Sellers, P J, Randall, D A, et al (1989), Effects of implementing the simple biosphere model in a general circulation model, *J Atmos Sci* 46(18) 2757–2782

Schimel, D S, Kittell, T G F, Knapp, A K, Seastedt, T R, Parton, W J, and Brown, V B (1991), Physiological interactions along resource gradients in a tallgrass prairie, *Ecology* 72 670–682

Seemann, J R, Sharkey, T D, Wang, J L, and Osmond, C B (1987), Environmental effects on photosynthesis, nitrogen-use efficiency, and metabolite pools in leaves of sun and shade plants, *Plant Physiol* 84 796–802

Sellers, P J (1985), Canopy reflectance, photosynthesis and transpiration, *Int J Remote Sens* 6 1335–1372

Sellers, P J (1987), Canopy reflectance, photosynthesis, and transpiration, II The role of Biophysics in the linearity of their interdependence, *Remote Sens Environ* 21 143–183

Sellers, P J, and Lockwood, J G (1981), Computer simula-

tion of the effects of differing crop types on the water balance of small catchments over long time periods, *Quart J Roy Meteorol Soc* 107 395–414

Sellers, P J, Mintz, Y, Sud, Y C, and Dalcher, A (1986), A simple biosphere model (SiB) for use within general circulation models, *J Atmos Sci* 43(6) 305–331

Sellers, P J, Hall, F G, Asrar, G, Strebel, D E, and Murphy, R E (1988), The First ISLSCP Field Experiment (FIFE) *Bull Am Meterol Soc* 69 22–27

Sellers, P J, Shuttleworth, J W, Dorman, J L, Dalcher A, and Roberts, J M (1989), Calibrating the simple biosphere model (SiB) for Amazonian tropical forest using field and remote sensing data Part 1 Average calibration with field data, *J Appl Meteorol* 28(8) 727–759

Tans, P P, Fung, I Y, and Takahashi, T (1990), Observational constraints on the global atmospheric CO_2 budget, *Science* 247 1431–1438

Terashima, I and Inouye, Y (1985), Vertical gradient in photosynthetic properties of spinach chloroplasts dependent on intra-leaf light environment, *Plant Cell Physiol* 26 781–785

Tucker, C J, Holben, B N, Elgin, J H, and McMurtrey, E (1981), Remote sensing of total dry matter accumulation in winter wheat, *Remote Sens Environ* 11 171–190

von Caemmerer, S, and Farquhar, G D (1985), Kinetics and activation of Rubisco and some preliminary modelling of RuP_2 pool sizes, in *Proceedings of the 1983 Conference at Tallinn* (J Vill, G Grishina, and A Laisk, Eds), Estonian Academy of Sciences, Tallinn, pp 46–58

Walters, M B, and Field, C B (1987), Photosynthetic light acclimation in two rainforest Piper species with different ecological amplitudes, *Oecologia* 72 449–456

Wong, S C, Cowan, I R and Farquhar, G D (1979), Stomatal conductance correlates with photosynthetic capacity, *Nature* 282 424–426